

Optimized Conformal Selection: Powerful Selective Inference After Conformity Score Optimization

Tian Bai¹ and Ying Jin²

¹Department of Mathematics and Statistics, McGill University

²Data Science Initiative and Department of Health Care Policy, Harvard University

Abstract

Model selection/optimization in conformal inference is challenging, since it may break the exchangeability between labeled and unlabeled data. We study this problem in the context of conformal selection, which uses conformal p-values to select “interesting” instances with large unobserved labels from a pool of unlabeled data, while controlling the FDR in finite sample. For validity, existing solutions require the model choice to be independent of the data used to construct the p-values and calibrate the selection set. However, when presented with many model choices and limited labeled data, it is desirable to (i) select the best model in a data-driven manner, and (ii) mitigate power loss due to sample splitting.

This paper presents OptCS, a general framework that allows valid statistical testing (selection) after flexible data-driven model optimization. We introduce general conditions under which OptCS constructs valid conformal p-values despite substantial data reuse and handles complex p-value dependencies to maintain finite-sample FDR control via a novel multiple testing procedure. We instantiate this general recipe to propose three FDR-controlling procedures, each optimizing the models differently: (i) selecting the most powerful one among multiple pre-trained candidate models, (ii) using all data for model fitting without sample splitting, and (iii) combining full-sample model fitting and selection. We demonstrate the efficacy of our methods via simulation studies and real applications in drug discovery and alignment of large language models in radiology report generation.

Keywords: Conformal prediction, conformal p-value, model selection, FDR control, sample splitting.

1 Introduction

Conformal inference is a versatile, distribution-free framework for predictive inference [Vovk et al., 2005]. Given any prediction model, it uses a conformity score to measure how well the outcomes “conform” to model predictions; it then leverages data exchangeability to deliver statistical evidence (p -value) for various tasks, including prediction set construction [Lei et al., 2018] and recent extensions in two-sample testing [Hu and Lei, 2024] and multiple testing [Bates et al., 2023, Jin and Candès, 2023c]. Its strength lies in its flexibility as a “wrapper” for valid inference, regardless of the model or score used. However, despite this flexibility, a common challenge is model selection: determining the optimal conformity score and/or prediction model to improve the performance for the specific statistical task at hand.

We study model selection in the context of model-free selective inference [Jin and Candès, 2023b], which aims to identify unlabeled samples with large unobserved labels while controlling selection errors. Formally, given labeled data $\{(X_i, Y_i)\}_{i=1}^n$ and unlabeled test samples $\{X_{n+j}\}_{j=1}^m$, the goal is to select a subset $\mathcal{S} \subseteq \{1, \dots, m\}$ of test samples such that most of them obey $Y_{n+j} > c_{n+j}$, where c_{n+j} are user-specified thresholds above which the outcomes are considered interesting. This is formalized by false discovery rate (FDR) control:

$$\text{FDR} := \mathbb{E} \left[\frac{\sum_{j=1}^m \mathbf{1}\{j \in \mathcal{S}, Y_{n+j} \leq c_{n+j}\}}{1 \vee |\mathcal{S}|} \right] \leq q, \quad (1)$$

where $q \in (0, 1)$ is a user-specified nominal level. Since the FDR measures the proportion of correctly selected instances, rigorous control of FDR is crucial for the trustworthiness of such prediction-driven screening and the efficiency of downstream investigations on the selected units (see below for representative applications).

Conformal selection [Jin and Candès, 2023c] addresses this problem by extending conformal inference ideas to multiple test samples; see also recent extensions to covariate shift [Jin and Candès, 2023b], online [Xu and Ramdas, 2024], and constrained settings [Wu et al., 2023, Huo et al., 2024, Wang et al., 2024], and applications to drug discovery [Bai et al., 2024] and large language models [Gui et al., 2024]. In a nutshell, given any conformity score, it offers an automatic pipeline to construct p -values using a set of labeled data (called calibration data) and determine the selection set by multiple testing. Its performance thus relies on the combined choice of the conformity score and prediction model, which we term the “model choice”.

To maintain FDR control, the model choice is required to be independent of the test and calibration data, akin to the celebrated split conformal prediction idea [Lei et al., 2018]. This constraint prevents practitioners from selecting models based on their observed performance, and often necessitates splitting labeled data for training, which may also compromise power. We illustrate the practical need for optimizing model selection without these limitations through two typical applications of conformal selection.

- **Drug discovery.** Early stages of drug discovery aim to find highly viable drug candidates—molecules, antibiotics, or proteins—with desirable biological properties [Szymański et al., 2011, Macarron et al., 2011]. Such tasks can be characterized by finding drug candidates $j \in \{1, \dots, m\}$ with $Y_{n+j} > c_{n+j}$ for certain unknown property Y_{n+j} and thresholds c_{n+j} . Given any model that predicts Y_{n+j} based on physical/chemical features X_{n+j} , conformal selection can be used to shortlist drug candidates with FDR control, enabling efficient pre-evaluation before costly validations [Jin and Candès, 2023c]. With numerous pretrained drug property prediction models by recent advances in empirical machine learning [Xiong et al., 2019, Li et al., 2021, Huang et al., 2020, Carracedo-Reboredo et al., 2021], it is desirable to use data at hand to determine the best one for an FDR-controlling drug discovery task.
- **LLM abstention.** Large language models (LLMs) show tremendous potential in high-stakes tasks such as generating radiology reports, but issues like hallucination and factual errors pose significant risks [Huang et al., 2023, Weidinger et al., 2021]. In this context, conformal selection can be used to select radiology images $j \in \{1, \dots, m\}$ for which the generated reports align with expert standards, represented by an unknown ‘alignment indicator’ $Y_{n+j} = 1$. Gui et al. [2024] trains a model (alignment predictor) that predicts Y_{n+j} based on features of LLM outputs X_{n+j} using images with human-expert reports (labeled training data), and applies conformal selection to select new images with “aligned” outputs using a separate calibration dataset. With various model choices for the alignment predictor, it becomes crucial to efficiently use the usually limited labeled data to optimize the selection performance.

The challenges in model selection have been more extensively studied in constructing conformal prediction sets for a single test point [Stutz et al., 2021, Yang and Kuchibhotla, 2024, Huang et al., 2024, Xie et al., 2024, Liang et al., 2024a]. First, selecting models based on their observed performance introduces a double-dipping bias, disrupting the exchangeability essential for validity [Liang et al., 2024a]. To address this, a popular strategy is to conduct model selection in a smaller, independent fold [Stutz et al., 2021, Yang and Kuchibhotla, 2024, Huang et al., 2024, Xie et al., 2024]. However, this needs additional sample splitting, which may compromise the power gain from model selection. While conformal selection inherits both challenges in optimizing model choices without violating FDR control, here with multiple test points, the limited data makes it even harder to design effective strategies, e.g., simulating the performance of individual models.

Our contributions. In this paper, we propose Optimized Conformal Selection (OptCS), a general framework for maintaining FDR-controlling sample selection while allowing flexible reuse of data for model optimization. We summarize our methodological contributions below.

- In Section 3, we present a general procedure (visualized in Figure 1) that encompasses all use cases of OptCS. We introduce permutation-based conditions for constructing p -values and multiple testing, which allow to build conformity scores (test statistics) through flexible data-dependent processes that

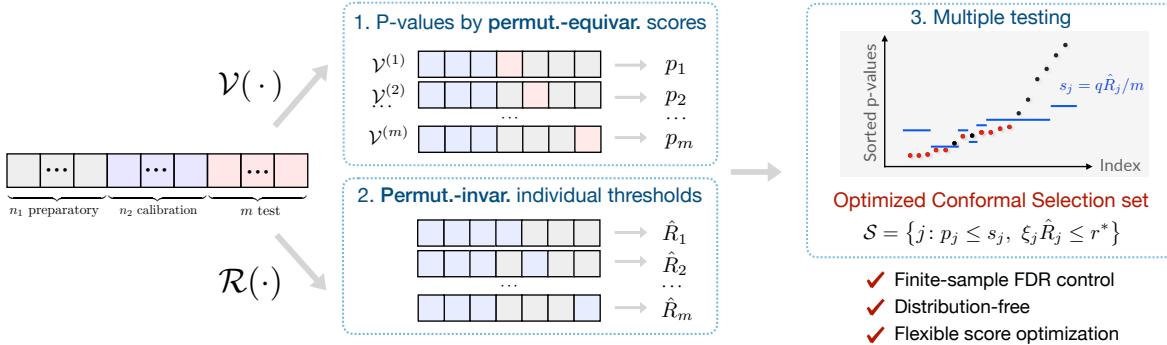


Figure 1: Overview of OptCS. (Optional) Split labeled data into preparatory and calibration sets. 1. P-value. We construct conformal p-values $\{p_j\}$ based on conformity scores from any data-dependent model optimization process $\mathcal{V}(\cdot)$ obeying a mild permutation-equivariance condition. 2. Selection threshold. We calibrate individual thresholds \hat{R}_j obeying a mild permutation-invariance condition. 3. Multiple testing. We combine $\{p_j\}$ and $\{\hat{R}_j\}$ to produce a selection set \mathcal{S} with finite-sample, distribution-free FDR control.

may involve all the data while controlling the FDR in screening for large-valued outcomes.

- In Section 4.1, we develop OptCS-MSel, an instantiation of OptCS that exploits power gain from selecting optimal model classes. It yields FDR-controlling conformal selection after adaptively selecting from multiple pre-trained models while permitting “double-dipping”-like behavior for model selection.
- In Section 4.2, we develop OptCS-Full, a second instantiation of OptCS that leverages all labeled data to fit a more accurate prediction model within a given model class (i.e., without model selection). OptCS-Full avoids the randomness and power loss in sample splitting, and can be viewed as a generalization of full conformal prediction [Vovk et al., 2005] to multiple testing contexts.
- In Section 4.3, we propose OptCS-Full-MSel, which combines the preceding two ideas to simultaneously exploit power gain from full-data training and model selection. It involves all labeled data for model training, selection, and constructing the selection set \mathcal{S} , and typically yields the highest power.

Figure 2 previews the performance of the three procedures with distinct model optimization strategies in our numerical experiments. Each strategy, applicable in different scenarios, significantly improves power upon baseline methods. Finally, we demonstrate the efficacy of the methods through numerical simulations in Section 5 and real applications in drug discovery and large language model abstention in Section 6.

Data and Code. Reproducibility code for both our simulation and real data experiment can be found at the Github repository <https://github.com/Tian-Bai/OptCS>.

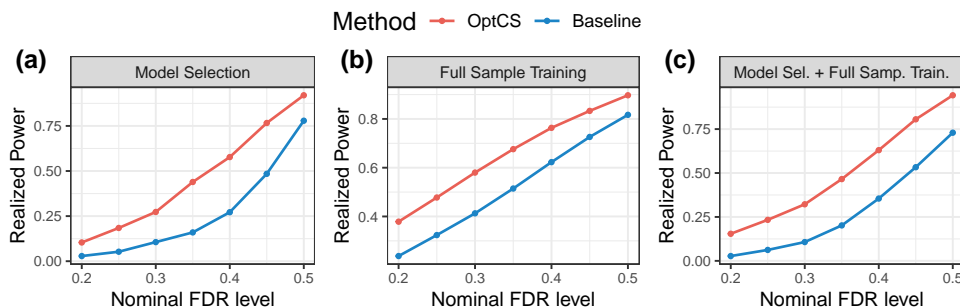


Figure 2: Preview of numerical results. Left: Performance of OptCS-MSel which selects from pre-trained models. Middle: Performance of OptCS-Full which leverages full data for model fitting with a given model class. Right: Performance of OptCS-Full-MSel which combines model selection and full-sample training.

2 Preliminaries

In this section, we first review the key ideas in the conformal selection framework [Jin and Candès, 2023c], and then discuss the challenges in optimizing the conformity score function, followed by a brief overview of related works in the field of selection inference and conformal inference.

2.1 Recap: Conformal selection

Assume access to a set of labelled data $\mathcal{D}_{\text{label}} = \{(X_i, Y_i)\}_{i=1}^n$ and a set of unlabeled test data $\mathcal{D}_{\text{test}} = \{X_{n+j}\}_{j=1}^m$ whose responses $\{Y_{n+j}\}_{j=1}^m$ are unobserved. Conformal selection begins by randomly splitting the labelled data $\mathcal{D}_{\text{label}}$ into two disjoint subsets, the training set $\mathcal{D}_{\text{train}} := \{(X_i, Y_i)\}_{i=1}^{n_1}$ and the calibration set $\mathcal{D}_{\text{calib}} := \{(X_i, Y_i)\}_{i=n_1+1}^n$. First, $\mathcal{D}_{\text{train}}$ is used to train a model and build a *monotone* conformity score function $V : \mathcal{X} \times \mathcal{Y} \rightarrow \mathbb{R}$ where \mathcal{X} and $\mathcal{Y} \subseteq \mathbb{R}$ represent the sample space of $\{X_i\}$ and $\{Y_i\}$, respectively.

Definition 1. A score function $V : \mathcal{X} \times \mathcal{Y} \rightarrow \mathbb{R}$ is monotone if $V(x, y) \leq V(x, y')$ whenever $y \leq y'$ for any $x \in \mathcal{X}$ and $y, y' \in \mathcal{Y}$.

The score function V can wrap around any prediction model (obtained in the training step), e.g., $V(x, y) = y - \hat{\mu}(x)$ where $\hat{\mu}(x)$ is a point prediction for y given x . Other popular choices include those based on quantile regression [Romano et al., 2019] and conditional cumulative distribution functions [Chernozhukov et al., 2021]. We then compute the calibration scores $V_i = V(X_{n_1+i}, Y_{n_1+i})$, $i = 1, \dots, n_2$, and test scores $\hat{V}_{n+j} = V(X_{n+j}, c_{n+j})$. These scores can be understood as “test statistics” for large outcomes, and we will use this term interchangeably. Conformal selection then builds a conformal p -value for each test point:

$$p_j = \frac{\sum_{i=n_1+1}^n \mathbb{1}\{V_i < \hat{V}_{n+j}\} + U_j \cdot (1 + \sum_{i=n_1+1}^n \mathbb{1}\{V_i = \hat{V}_{n+j}\})}{n_2 + 1},$$

where $U_j \stackrel{\text{i.i.d.}}{\sim} \text{Unif}([0, 1])$ is a random variable for tie-breaking, and $n_2 = n - n_1$. Intuitively, a small p -value suggests that \hat{V}_{n+j} is unusually large compared to $\{V_i\}$, indicating that the corresponding Y_{n+j} is likely to exceed c_{n+j} , i.e., the unobserved label is “of interest”. Formally, $\mathbb{P}(p_j \leq t, Y_{n+j} \leq c_{n+j}) \leq t$ for all $t \in [0, 1]$.

The selection set \mathcal{S} is then obtained by applying the Benjamini-Hochberg (BH) procedure [Benjamini and Hochberg, 1995] to $\{p_j\}_{j=1}^m$ at the nominal FDR level q . As long as each test point (X_{n+j}, Y_{n+j}) is exchangeable with the calibration data $\{(X_i, Y_i)\}_{i=n_1+1}^n$, it is shown in Jin and Candès [2023c] that \mathcal{S} obeys the FDR control (1) in finite samples.

From now on, we refer to this procedure as Split Conformal Selection (SCS) for expositional convenience. As suggested by Jin and Candès [2023c], we will exclusively focus on powerful “clipped”-type scores below.

Assumption 1. The thresholds $\{c_i\}_{i=1}^n$ are observed for the labeled data, such that $\{(X_i, c_i, Y_i)\}_{i=1}^{n+m}$ are exchangeable across $i \in [n + m]$. All the score functions considered are “clipped”-type scores which obey $V(X_i, Y_i) = V(X_i, c_i)$ when $Y_i \leq c_i$.

With observed $\{c_i\}_{i=1}^n$, any monotone score function can be translated to a clipped version with strictly higher power. Besides higher power, the property that $V(X_i, Y_i) = V(X_i, c_i)$ when $Y_i \leq c_i$ is crucial for flexible score optimization without observing the true test labels. Finally, the score function implicitly depends on the thresholds, i.e., $V(x, y, c)$, yet we suppress the dependence on c for notational simplicity.

2.2 Challenges in optimizing conformity score function

We take a moment to review the theoretical underpinning of SCS and discuss the challenges in preserving FDR control while optimizing the score function with substantial data reuse. Readers may skip this subsection without missing key concepts.

At a high level, the FDR control of SCS relies on two facts:

- (i) *Valid p-values*: when \widehat{V}_{n+j} is replaced with the unobserved $V(X_{n+j}, Y_{n+j})$, the conformal p -value follows a uniform distribution due to exchangeability. Thus, a small value of p_j indicates evidence for $\widehat{V}_{n+j} < V(X_{n+j}, Y_{n+j})$ and hence $Y_{n+j} > c_{n+j}$ due to monotonicity of the function V .
- (ii) *Favorable p-value dependence*: while the conformal p -values are dependent since they use the same set of calibration data, a second crucial fact is that they are positively dependent [Bates et al., 2023, Jin and Candès, 2023c], which ensures FDR control with the BH procedure.

Ensuring the independence between the model choice V and the data it applies to (i.e., $\mathcal{D}_{\text{calib}} \cup \mathcal{D}_{\text{test}}$) is essential for both facts above, which can be disrupted when V or the “test statistic” is chosen with data.

We illustrate this point with a naive attempt to optimize the score function. Suppose there are candidate score functions $\{V(\cdot, \cdot; k): \mathcal{X} \times \mathcal{Y} \rightarrow \mathbb{R}\}_{k=1}^K$ obtained in the training fold. A simple idea is to run SCS with each score and choose the one that leads to the largest selection set. Namely, one selects

$$\widehat{k} = \operatorname{argmax}_{k \in [K]} |\mathcal{S}(k)|,$$

where $\mathcal{S}(k)$ is the output of SCS with the k -th score $V(\cdot, \cdot; k)$. The final selection set is $\mathcal{S} = \mathcal{S}(\widehat{k})$, which is equivalent to applying the BH procedure to p -values (assuming no ties for simplicity)

$$p_j = \frac{\sum_{i=n_1+1}^n \mathbb{1}\{V(X_i, Y_i; \widehat{k}) < V(X_{n+j}, c_{n+j}; \widehat{k})\} + 1}{n_2 + 1}. \quad (2)$$

Note that \widehat{k} depends on $\mathcal{D}_{\text{calib}}$ and (X_{n+j}, c_{n+j}) in a non-symmetric way. Thus, the scores $V(X_i, Y_i; \widehat{k})$ and $V(X_{n+j}, Y_{n+j}; \widehat{k})$ are no longer exchangeable, violating the validity of p -values (2). It is also difficult to justify their positive dependence for FDR control, since \widehat{k} is a complex function of the calibration and test data. Indeed, we will observe drastic violation of FDR by such “arbitrary” double-dipping in our experiments.

In general, optimizing the conformity score function inherently introduces substantial data reuse, such as by inspecting the selection performance or by avoiding sample splitting. Just as in this simple example, such data reuse often invalidates individual p -values and complicates FDR control due to intricate dependency. To address these challenges, our approach is to (i) construct valid p -values after score optimization, and (ii) conduct multiple testing with FDR control under less stringent requirements on the p -value dependence.

2.3 Related works

This work builds upon the conformal selection framework [Jin and Candès, 2023c] for the model-free selective inference problem, with recent extensions to settings with covariate shift [Jin and Candès, 2023b], online selection [Xu and Ramdas, 2024], and selection with objectives and constraints [Wu et al., 2023, Huo et al., 2024, Wang et al., 2024]. The FDR control it offers ensures the reliability and efficiency of decision-making and scientific discovery processes that use machine learning prediction models for data screening, such as representative applications in compound screening for drug discovery [Bai et al., 2024, Jin and Candès, 2023a] and selecting trusted outputs from large language models [Gui et al., 2024]. These applications motivate the need to select a best-performing conformity score while maintaining rigorous FDR control.

This work adds to the literature on model selection and optimization in conformal inference to enhance downstream task performance. This literature covers the tasks of (i) prediction set construction for a single test point and (ii) selection of multiple test points. In (i), while earlier works propose score functions based on theoretical justification [Romano et al., 2019, 2020], while recent approaches perform data-driven score selection by further splitting the data and conduct model selection/optimization on a separate data fold to maintain validity [Stutz et al., 2021, Yang and Kuchibhotla, 2024, Huang et al., 2024, Xie et al., 2024, Liang et al., 2024a]. Besides, Liang et al. [2024a] studies problem (i) without extra sample splitting by maintaining permutation invariance to the calibration and test point. While related, our techniques are quite different since we consider selecting multiple data points with FDR control, instead of prediction set for one test point. Works for task (ii) are limited to the outlier detection setting [Liang et al., 2024b, Marandon et al., 2024], wherein the strategies for developing better scores are pre-determined instead of being data-driven.

To control the FDR with complicated dependence structure, our general approach is to calibrate individual selection criteria for p-values. This generalizes the strategy in [Jin and Candès \[2023b\]](#) used to address complicated dependence between weighted conformal p-values due to reweighting, which was extended by [Xu and Ramdas \[2024\]](#) to online settings. However, our construction is more general and serves distinct purposes. It can also be viewed as an extension of conditional calibration [[Fithian and Lei, 2022](#)] yet without Monte-Carlo calibration of the thresholds due to the exchangeable structure in conformal inference.

2.4 Notations

Throughout the paper, we denote the full observations as $Z_i = (X_i, Y_i)$ for $i = 1, 2, \dots, n+m$ and the partial observations as $\hat{Z}_{n+j} = (X_{n+j}, c_j)$ for $j = 1, 2, \dots, m$. For any set A , we write $[A]$ as its unordered version, which provides the same information as the order statistics of values in A . For any integer $m \in \mathbb{N}$, we denote $[m] := \{1, 2, \dots, m\}$. For a vector $\mathbf{z} \in \mathbb{R}^d$, we denote z_i as the i -th element. For a matrix $M \in \mathbb{R}^{d_1 \times d_2}$, we denote M_{ij} as the element on the i -th row and j -th column, $M_{i,:}$ as the i -th row vector, and $M_{:,j}$ the j -th column vector. For values a_1, \dots, a_n , we sometimes write $a_{1:n} = (a_1, \dots, a_n)$.

3 Optimized Conformal Selection

We begin by introducing a general procedure that encompasses all use cases of OptCS, including model selection and full-sample model training and/or selection. The entire workflow consists of three steps:

- *Step 1: P-value construction.* We introduce a novel approach to construct valid conformal p-values using data-driven score functions, allowing for flexible model selection and optimization.
- *Step 2: Calibration of selection criteria.* As preparation for multiple testing, we calibrate individual selection criteria for the p-values using “auxiliary selection sizes”. This step addresses the complex dependencies among the p-values obtained in Step 1 that may arise from data-driven score functions.
- *Step 3: Multiple testing.* Finally, we develop a multiple testing procedure that leverages the p-values and auxiliary selection sizes to construct the final selection set, ensuring finite-sample FDR control.

The high-level idea of OptCS is to “individualize” the p -values and selection criteria, constructed via slightly different model optimization processes for each test point. The key to validity is to ensure the optimization process for the j -th test sample is symmetric with respect to this sample and the calibration data, thereby separating the information used in the p -value and in the model optimization process for rigorous FDR control. This allows considerable flexibility in adapting to the data at hand, both in constructing powerful test statistics (via the score-generating functional) and in calibrating the multiple testing procedure (via the auxiliary selection sizes). We detail these steps in [Section 3.1](#), followed by the general theoretical guarantee in [Section 3.2](#). Concrete use cases of OptCS will be introduced in [Section 4](#).

3.1 General procedure

Step 1: P-values. The first innovation of OptCS is a general construction of valid conformal p-values with data-driven score functions. By “data-driven”, we mean the choice of scores may depend on the calibration and test data. To enable such flexibility while ensuring the validity of the resulting p-values, we introduce the notion of score-generating functional, which allows to use individual score functions for each test point.

Definition 2 (Score-generating functional). *A score-generating functional is a function $\mathcal{V} : (\mathcal{X} \times \mathcal{Y})^{n+m} \rightarrow \mathbb{R}^{m \times (n_2+m)}$ with $n_1, n_2, n, m \in \mathbb{N}$, and $n = n_1 + n_2$. For notational simplicity, we denote $\mathcal{V}^{(j)} : (\mathcal{X} \times \mathcal{Y})^{n+m} \rightarrow \mathbb{R}^{n_2+m}$ such that $\mathcal{V}^{(j)}(\mathbf{z}) = \mathcal{V}(\mathbf{z})_{j,:}$ for any $\mathbf{z} \in (\mathcal{X} \times \mathcal{Y})^{n+m}$.*

[Figure 3](#) illustrates the inputs and outputs of a score-generating functional. We refer to the first n_1 labeled samples as preparatory data and the subsequent n_2 labeled samples as calibration data. The calibration data will be assigned scores to compare with test scores for p -value construction. This separation simplifies

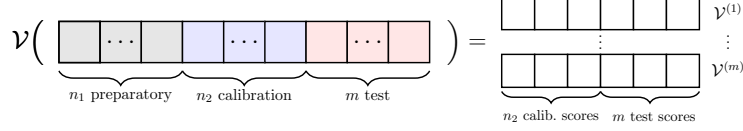


Figure 3: Visualization of a score-generating functional.

descriptions of preparatory steps like model pre-training (see Section 4.1 for such a scenario). One may simply take $n_1 = 0$ to involve all the labeled data in both score generating and calibration. In the full-data procedures in Sections 4.2 and 4.3, the preparatory data will always be used in training, yet excluding them from calibration reduces the number of required model fits. Finally, the last m inputs represent $\{\widehat{Z}_{n+j}\}_{j=1}^m$ with unknown responses. The output of \mathcal{V} is an $m \times (n_2 + m)$ matrix. Each row $\mathcal{V}^{(j)}$ will be used to construct the j -th p -value. It can be viewed as a process that generates a score function $V^{(j)}: \mathcal{X} \times \mathcal{Y} \rightarrow \mathbb{R}$, which is then applied to the $(n_2 + m)$ calibration and test inputs to obtain their numerical scores in the j -th row.

Remark 3.1. Definition 2 strictly generalizes the concept of score functions in SCS. As introduced in Section 2, SCS computes the calibration scores $\{V_i\}_{i=n_1+1}^n$ and test scores $\{\widehat{V}_{n+j}\}_{j=1}^m$ using a pre-determined score function V . This is a special case with $\mathcal{V}^{(j)}(\mathbf{z}) \equiv (V_1, \dots, V_{n_2}, \widehat{V}_{n+1}, \dots, \widehat{V}_{n+m})$.

Intuitively, \mathcal{V} encapsulates all the model selection/optimization operations to search for a powerful score (test statistic). For instance, it may include a process where SCS is applied to the calibration and test data with multiple candidate pre-determined score functions, and one of them is chosen based on the selection performance. It may also include a training process that involves all the labeled and unlabeled data.

Given data $Z_{1:n_1}$, $Z_{n_1+1:n}$, and $\widehat{Z}_{n+1:n+m}$, we denote the generated scores as

$$(V_{n_1+1}^{(j)}, \dots, V_n^{(j)}, \widehat{V}_{n+1}^{(j)}, \dots, \widehat{V}_{n+m}^{(j)}) := \mathcal{V}^{(j)}(Z_{1:n_1}, Z_{n_1+1:n}, \widehat{Z}_{n+1:n+m}). \quad (3)$$

We then compute the conformal p -values in the same way as conformal selection:

$$p_j = \frac{1 + \sum_{i=n_1+1}^n \mathbb{1}\{V_i^{(j)} \leq \widehat{V}_{n+j}^{(j)}\}}{n_2 + 1}. \quad (4)$$

The validity of each p_j only requires each set of scores (3) in $\mathcal{V}^{(j)}$ to be monotone and permutation equivariant to the calibration data and the j -th test point, formalized in the two definitions below.¹ By associating the construction of each p -value with an individual score-generating process, it is much easier to fulfill these requirements with flexibility by designing each individual process.

Definition 3 (Monotonicity for the null). *A score-generating functional $\mathcal{V}: (\mathcal{X} \times \mathcal{Y})^{n_1+n_2+m} \rightarrow \mathbb{R}^{m \times (n_2+m)}$ is monotone for the j -th null, if for any $z'_{1:n_1} \in (\mathcal{X} \times \mathcal{Y})^{n_1}$, $z_{1:n_2} \in (\mathcal{X} \times \mathcal{Y})^{n_2}$, $\widehat{z}_{n+1:n+m} \in (\mathcal{X} \times \mathcal{Y})^m$, where $z_i = (x_i, y_i)$, $\widehat{z}_{n+j} = (x_{n+j}, c_{n+j})$, and $z_{n+j} = (x_{n+j}, y_{n+j}) \in \mathcal{X} \times \mathcal{Y}$, whenever $y_{n+j} \leq c_{n+j}$, it holds that*

$$\mathcal{V}^{(j)}(z'_{1:n_1}, z_{1:n_2}, \widehat{z}_{n+1:n+j-1}, \widehat{z}_{n+j}, \widehat{z}_{n+j+1:n+m})_{n_2+j} \geq \mathcal{V}^{(j)}(z'_{1:n_1}, z_{1:n_2}, \widehat{z}_{n+1:n+j-1}, z_{n+j}, \widehat{z}_{n+j+1:n+m})_{n_2+j},$$

and for any $\ell \neq j$, $\ell \in [n_2 + m]$,

$$\mathcal{V}^{(j)}(z'_{1:n_1}, z_{1:n_2}, \widehat{z}_{n+1:n+\ell-1}, \widehat{z}_{n+\ell}, \widehat{z}_{n+\ell+1:n+m})_{\ell} = \mathcal{V}^{(j)}(z'_{1:n_1}, z_{1:n_2}, \widehat{z}_{n+1:n+\ell-1}, z_{n+\ell}, \widehat{z}_{n+\ell+1:n+m})_{\ell}.$$

Definition 4 (Permutation equivariance). *We say a score-generating functional $\mathcal{V}: (\mathcal{X} \times \mathcal{Y})^{n_1+n_2+m} \rightarrow \mathbb{R}^{m \times (n_2+m)}$ is permutation equivariant if for all $j \in [m]$, and for any $z'_{1:n_1} \in (\mathcal{X} \times \mathcal{Y})^{n_1}$, $z_{1:(n_2+m)} \in (\mathcal{X} \times \mathcal{Y})^{n_2+m}$, and any permutation $\pi: \{1, \dots, n_2, n_2 + j\} \rightarrow \{1, \dots, n_2, n_2 + j\}$, it holds that*

$$\mathcal{V}^{(j)}(z'_{1:n_1}, z_{1:n_2}, z_{n_2+1}, \dots, z_{n_2+j}, \dots, z_{n_2+m})_{\pi(i)} = \mathcal{V}^{(j)}(z'_{1:n_1}, z_{\pi(1:n_2)}, z_{n_2+1}, \dots, z_{\pi(n_2+j)}, \dots, z_{n_2+m})_i.$$

¹In the general case where \mathcal{V} is a randomized algorithm, we require Definition 3 to hold conditional on the randomness in the algorithm, while Definition 4 to hold in a distributional sense, i.e., $=$ could be replaced by $\stackrel{d}{=}$.

The above definitions impose two intuitive requirements on the (j -th set of) generated scores which extend upon SCS. Definition 3 is a generalization of the simple idea that higher Y values should lead to higher scores. Technically, it ensures the ordering of scores informs the ordering of Y_{n+j} and c_{n+j} , extending Definition 1 to data-dependent scores. Definition 4 posits that permuting the $(n_2 + 1)$ inputs moves the positions of their output score values accordingly without changing their values. It ensures that our p -values behave correctly under the null hypothesis despite the data-driven search for powerful test statistics.

While we write the two conditions in a general form to cover all use cases, intuitively, our methods meet these conditions by setting $V_i^{(j)} = V(X_i, Y_i; \hat{\mu})$, where V is monotone in y given any fitted model $\hat{\mu}$, and $\hat{\mu}$ is obtained from a process that is permutation invariant to $\{Z_i\}_{i=n_1+1}^n$ and the j -th test point. Later, we will construct \mathcal{V} in concrete scenarios and show how these conditions are met in each of them.

Our p -values (4) are “valid” in the same sense as in SCS under the above two conditions. However, the dependence among these p -values can be intricate due to the flexible score-generating process; e.g., they might not be PRDS [Benjamini and Yekutieli, 2001]. We thus need additional techniques for FDR control.

Step 2: Calibrate selection criteria. To handle dependency, our second innovation is to calibrate individual selection criteria for the p -values via “auxiliary selection sizes”. These variables are conditionally independent of our p -values; as such, they guide multiple testing without interrupting the information contained in the p -values. They are defined via a function that satisfies a permutation invariance condition.

Definition 5 (Permutation invariance under the null). *We say a function $\mathcal{R}: (\mathcal{X} \times \mathcal{Y})^{m+n} \rightarrow (\mathbb{R}^+)^m$ is permutation invariant under the j -th null if for any $z'_{1:n_1} \in (\mathcal{X} \times \mathcal{Y})^{n_1}$, $z_{1:n_2} \in (\mathcal{X} \times \mathcal{Y})^{n_2}$, $\hat{z}_{n+1:n+m} \in (\mathcal{X} \times \mathcal{Y})^m$, and any $z_{n+j} = (x_{n+j}, y_{n+j})$ obeying $y_{n+j} \leq c_{n+j}$, it holds that*

$$\mathcal{R}(z'_{1:n_1}, z_{1:n_2}, \hat{z}_{n+1:n+j-1}, \hat{z}_{n+j}, \hat{z}_{n+j+1:n+m})_j \geq \mathcal{R}_0(z'_{1:n_1}, z_{1:n_2}, \hat{z}_{n+1:n+j-1}, z_{n+j}, \hat{z}_{n+j+1:n+m})_j, \quad (5)$$

for some function $\mathcal{R}_0: (\mathcal{X} \times \mathcal{Y})^{n+m} \rightarrow (\mathbb{R}^+)^m$ obeying

$$\mathcal{R}_0(z'_{1:n_1}, z_{1:n_2}, z_{n+1}, \dots, z_{n+j}, \dots, z_{n+m})_j = \mathcal{R}_0(z'_{1:n_1}, z_{\pi(1:n_2)}, z_{n+1}, \dots, z_{\pi(n+j)}, \dots, z_{n_2+m})_j \quad (6)$$

for any permutation $\pi: \{1, \dots, n_2, n+j\} \rightarrow \{1, \dots, n_2, n+j\}$.

The key intuition behind the permutation invariance condition is that \mathcal{R} only use auxiliary information in the unordered set of $\{Z_i\}_{i=n_1+1}^n$ and the j -th test point. This is similar to how we keep the search of scores (test statistics) auxiliary to the ordering of data (ensured by permutation equivariance in Definition 4).

We define the auxiliary selection sizes as the output of such a functional \mathcal{R} :

$$(\hat{R}_1, \dots, \hat{R}_m) := \mathcal{R}(Z_{1:n_1}, Z_{n_1+1:n}, \hat{Z}_{n+1:n+m}). \quad (7)$$

While the permutation invariance condition is the only requirement, we will see later in Remark 3.4 that, when considering subsequent multiple testing, an ideal choice of \hat{R}_j is to mimic the selection set obtained by applying the BH procedure to p -values in (4).

Step 3: Multiple testing. Given the p -values (4) and the auxiliary selection sizes (7), we compute preliminary selection thresholds $s_j := q\hat{R}_j/m$, and construct the final selection set following Jin and Candès [2023b], Fithian and Lei [2022]:

$$\mathcal{S} = \{j: p_j \leq s_j, \xi_j \hat{R}_j \leq r^*\}, \quad \text{where } r^* := \max \left\{ r: \sum_{j=1}^m \mathbf{1} \{p_j \leq s_j, \xi_j \hat{R}_j \leq r\} \geq r \right\}, \quad (8)$$

with three options for $\{\xi_j\}$: (a) *Heterogeneous pruning*: independently generate $\{\xi_j\} \stackrel{\text{i.i.d.}}{\sim} \text{Unif}[0, 1]$; (b) *Homogeneous pruning*: set $\xi_j \equiv \xi$ for an independent $\xi \sim \text{Unif}[0, 1]$; (c) *Deterministic pruning*: set $\xi_j \equiv 1$.

Here, options (a,b) introduces external randomness that “smoothes” the pruning step. In our numerical experiments, the extra randomness in (a,b) improves both the power and stability of the final selection set upon (c), consistent with the observations in Jin and Candès [2023b]. The general procedure of OptCS is summarized in Algorithm 1.

Algorithm 1 Optimized Conformal Selection (General procedure)

Input: Labeled data $\{(X_i, Y_i)\}_{i=1}^n$, test data $\{X_{n+j}\}_{j=1}^m$, thresholds $\{c_{n+j}\}_{j=1}^m$, FDR target $q \in (0, 1)$, score-generating functional $\mathcal{V}(\cdot)$, auxiliary selection function $\mathcal{R}(\cdot)$, pruning method $\text{prune} \in \{\text{homo}, \text{hete}, \text{dtm}\}$.

- 1: (Optional) Split labeled data into preparatory data $\{(X_i, Y_i)\}_{i=1}^{n_1}$ and calibration data $\{(X_i, Y_i)\}_{i=n_1+1}^n$
- 2: **for** $j = 1, \dots, m$ **do**
- 3: Compute conformity scores $\{V_i^{(j)}\}_{i=n_1+1}^n$ and $\{\widehat{V}_{n+j}^{(j)}\}_{j=1}^m$ via (3). // Sub-routine 1
- 4: Compute p-value p_j via (4).
- 5: Compute auxiliary selection size \widehat{R}_j via (7). // Sub-routine 2
- 6: Set $\xi_j \equiv \xi \sim \text{Unif}([0, 1])$ if $\text{prune} = \text{homo}$, $\xi_j \stackrel{\text{i.i.d.}}{\sim} \text{Unif}([0, 1])$ if $\text{prune} = \text{hete}$, $\xi_j \equiv 1$ if $\text{prune} = \text{dtm}$.
- 7: **end for**
- 8: Compute selection set \mathcal{S} following (8).

Output: Selection set \mathcal{S} .

3.2 Theoretical guarantee

Our main theoretical result establishes finite-sample FDR control of OptCS, provided that the score-generating functional $\mathcal{V}(\cdot)$ and the auxiliary selection function $\mathcal{R}(\cdot)$ obey the appropriate conditions. The proof of Theorem 3.2 is in Appendix B.1.

Theorem 3.2. *Suppose for all $j \in [m]$, the following conditions hold:*

- (1) $(Z_1, \dots, Z_n, Z_{n+j})$ is exchangeable given $\{\widehat{Z}_{n+\ell}\}_{\ell \neq j}$;
- (2) the score-generating functional \mathcal{V} is monotone and permutation equivariant (Definitions 3 and 4);
- (3) the auxiliary selection functional $\mathcal{R}(\cdot)$ is permutation invariant under the j -th null (Definition 5).

Then, for any nominal FDR level $q \in (0, 1)$ and any pruning method, the output \mathcal{S} of OptCS obeys FDR control (1) in finite sample, where the expectation is taken over both the calibration and test data.

We now provide some intuitions and intermediate technical ideas for Theorem 3.2. At a high level, all “nuisance” steps, including model optimization and auxiliary threshold calculation, are conducted in a way such that the conformal p-values remain valid (i.e. uniformly distributed) conditional on them. In particular, this is achieved by the permutation equivariance of conformity scores and the permutation invariance of \widehat{R}_j . All these support the use of OptCS across a wide range of applications, as we will see in the next section.

To begin with, under any pruning option, we obtain the following decomposition of FDR. Lemma 3.3 adapts Lemma C.1 of Jin and Candès [2023c], and we include a proof in Appendix B.5 for completeness.

Lemma 3.3 (FDR decomposition). *Under any of the three pruning options, the output of Algorithm 1 obeys*

$$\text{FDR} \leq \sum_{j=1}^m \mathbb{E} \left[\frac{\mathbb{1}\{p_j \leq q\widehat{R}_j/m, Y_{n+j} \leq c_{n+j}\}}{\widehat{R}_j} \right]. \quad (9)$$

It thus suffices to ensure that each expectation in the summation (9) is controlled. We achieve so by showing that the p-value is uniformly distributed conditional on \widehat{R}_j on the null event. More specifically, let $[\mathcal{Z}_j] = [Z_{n_1+1}, \dots, Z_n, Z_{n+j}]$ be the unordered set of the $(n_2 + 1)$ full observations, and define \bar{R}_j as the j -th element of $\mathcal{R}_0(Z_{1:n_1}, Z_{n_1+1:n}, \widehat{Z}_{n+1:n+j-1}, Z_{n+j}, \widehat{Z}_{n+j+1:n+m})$. Under the conditions of Theorem 3.2, this is a consequence of the following two facts:

- $\mathbb{P}(p_j \leq t, Y_{n+j} \leq c_{n+j} \mid [\mathcal{Z}_j]) \leq t$ for all $t \in [0, 1]$ that is measurable with respect to $[\mathcal{Z}_j]$.
- $Y_{n+j} \leq c_{n+j}$ implies $\widehat{R}_j = \bar{R}_j$, and \bar{R}_j is measurable with respect to $[\mathcal{Z}_j]$.

Finally, we remark that the design of \widehat{R}_j should aim to approximate the selection size of applying the BH procedure to our p-values (4) while perserving the permutation invariance property.

Remark 3.4 (Design principle of \widehat{R}_j). Let \mathcal{S}_{BH} be the selection set of the BH procedure applied to $\{p_j\}$ in (4) at the same nominal level q . Then, we can show that the output of OptCS obeys $\mathcal{S} \subseteq \mathcal{S}_{\text{BH}}$. In addition, if $R_j \equiv |\mathcal{S}_{\text{BH}}|$ for all $j \in [m]$, then $\mathcal{S} = \mathcal{S}_{\text{BH}}$ under all three pruning options. See Appendix A.1 for a formal result. Thus, an intuitive idea is that R_j should approximate \mathcal{S}_{BH} in a permutation invariant fashion. We will follow this principle in our concrete instantiations of OptCS in the next section. In some special cases, the output of BH itself obeys Definition 5 hence no pruning is needed.

4 Instantiations of OptCS

In this section, we specify the construction of $\mathcal{V}(\cdot)$ and $\mathcal{R}(\cdot)$ in Algorithm 1, which leads to several concrete instantiations of OptCS with various purposes. Each of them represents an approach to constructing or selecting powerful test statistics (scores) while maintaining the theoretical guarantees in Section 3.

In a nutshell, we exploit two ways model optimization can improve power: (i) select the most powerful model among multiple choices, and (ii) use all labeled data for model fitting by avoiding sample splitting. Section 4.1 proposes OptCS-MSel which allows (i) when multiple pre-trained models are available. Section 4.2 proposes OptCS-Full which allows (ii) when a training model class is given. Finally, Section 4.3 proposes OptCS-Full-MSel which simultaneously achieves (i) and (ii) with multiple candidate model classes.

4.1 OptCS-MSel: Model selection over trained models

The first scenario we consider is when multiple pre-trained models have been obtained in a separate training stage, and a scientist aims to use data at hand to select the best model among them and produce an FDR-controlling selection set. This is suitable, for instance, in many drug discovery tasks where pre-trained models for drug properties are available to use yet too costly to retrain.

Following the notations in Section 2.2, there are K candidate scores $\{V(\cdot, \cdot; k) : \mathcal{X} \times \mathcal{Y} \rightarrow \mathbb{R}\}_{k=1}^K$ independent of the calibration and test points. Without loss of generality, we assume they are obtained with the fold $\{(X_i, Y_i)\}_{i=1}^{n_1}$, independent of the calibration data $\{(X_i, Y_i)\}_{i=n_1+1}^n$. Also recall $V_i(k) = V(X_i, Y_i; k)$ and $\widehat{V}_{n+j}(k) = V(X_{n+j}, c_{n+j}; k)$ are conformity scores using each model $k \in [K]$.

As we discussed in Section 2.2, greedily selecting the score function $k \in [K]$ that results in the largest selection set in SCS invalidates FDR control. In contrast, OptCS restores validity with a slightly modified procedure. The key idea is to select a model separately for each $j \in [m]$, each in a “greedy” yet permutation-invariant fashion. This selected model will be used to construct p_j and its auxiliary selection size \widehat{R}_j . In this way, we ensure that the model selection process does not bias the p-values, thus maintaining FDR control.

For each $j \in [m]$, we will construct a permutation-invariant estimate of the SCS output using the k -th model, denoted as $\mathcal{S}_j(k)$. Then, we greedily select $\widehat{k}_j = \operatorname{argmax}_k |\mathcal{S}_j(k)|$, and construct the functional \mathcal{V} via

$$\mathcal{V}^{(j)}(Z_1, \dots, Z_n, \widehat{Z}_{n+1}, \dots, \widehat{Z}_{n+m}) := \left(V_{n_1+1}(\widehat{k}_j), \dots, V_n(\widehat{k}_j), \widehat{V}_{n+1}(\widehat{k}_j), \dots, \widehat{V}_{n+m}(\widehat{k}_j) \right) \quad (10)$$

in Line 3 of Algorithm 1, as well as the auxiliary selection sizes $\widehat{R}_j = |\mathcal{S}_j(\widehat{k}_j)|$ in Line 5 of Algorithm 1. We visualize the comparison between OptCS and the naive approach in Figure 4.

We now specify $\widehat{\mathcal{S}}_j(k)$ for each model index $k \in [K]$. It is the output of the BH procedure applied to a set of slightly modified p-values $\{\widehat{p}_\ell^{(j)}(k)\}_{\ell \neq j} \cup \{0\}$ at the nominal level q , where

$$\widehat{p}_\ell^{(j)}(k) = \frac{\sum_{i \in \mathcal{I}_{\text{calib}}} \mathbf{1}\{V_i(k) \leq \widehat{V}_{n+\ell}(k)\} + \mathbf{1}\{\widehat{V}_{n+j}(k) \leq \widehat{V}_{n+\ell}(k)\}}{n_2 + 1}, \quad \ell \in [m], \ell \neq j. \quad (11)$$

Note that $\{\widehat{p}_\ell^{(j)}(k)\}_{\ell \neq j}$ are very close to the conformal p-values in SCS using the k -th score function, except the introduction of $\mathbf{1}\{\widehat{V}_{n+j}(k) \leq \widehat{V}_{n+\ell}(k)\}$ to preserve permutation invariance.

The following result, whose proof is in Appendix B.2, ensures that \mathcal{V} and \widehat{R}_j satisfy the conditions required by OptCS, and thus it ensures finite-sample FDR control by Theorem 3.2.

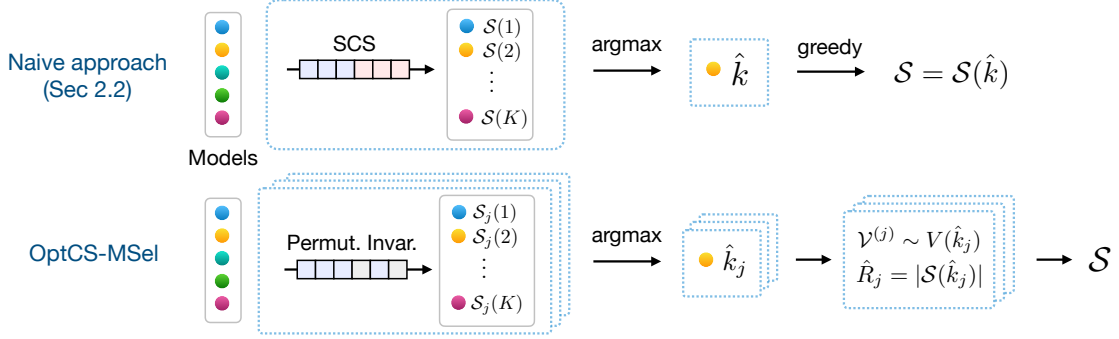


Figure 4: OptCS-MSel modifies the naive approach in Section 2.2 by individual model selection for each test point, replacing SCS in the evaluation step with a similar quantity $\mathcal{S}_j(\cdot)$ that is permutation invariant to the calibration data and the j -th test point. The selected models are used to calibrate the final selection set.

Proposition 4.1. *The score-generating functional \mathcal{V} and auxiliary selection function \mathcal{R} defined in OptCS-MSel obey Definitions 3, 4 and Definition 5. Therefore, the output of OptCS-MSel obeys $\text{FDR} \leq q$.*

4.2 OptCS-Full: Conformal selection without data splitting

In this part, we introduce OptCS-Full, a variant of OptCS that avoids sample splitting in conformal selection when model training with labeled data is needed. We will set aside the model selection issue and consider a fixed model class for the conformity score. That is, the prediction model will be trained through a given process, and the conformity score wraps around this model in a given fashion. The goal is to improve the scores/test statistics by training a more accurate model with more labeled data. A third method that simultaneously conducts model training and model selection will be studied in the next part.

For clarity, we represent the training process via an algorithm \mathcal{A} that takes as input a set of labeled data and output a trained model, e.g., $\mathcal{A}: \cup_{N \geq 0} (\mathcal{X} \times \mathcal{Y})^N \rightarrow \{\text{measurable functions } \hat{\mu}: \mathcal{X} \rightarrow \mathcal{Y}\}$. Of course, the output can be more general than a mapping from \mathcal{X} to \mathcal{Y} . For instance, it might consist of a point prediction model and a variance estimator to be used in the score function, or a conditional c.d.f. function. Here, we use $\hat{\mu}$ to refer to the trained output for simplicity. We require that \mathcal{A} treats the input data symmetrically:²

$$\mathcal{A}((x_1, y_1), \dots, (x_N, y_N)) = \mathcal{A}((x_{\pi(1)}, y_{\pi(1)}), \dots, (x_{\pi(N)}, y_{\pi(N)})) \quad (12)$$

for any permutation $\pi: [N] \rightarrow [N]$. The score function wraps around a fitted model $\hat{\mu}: \mathcal{X} \rightarrow \mathcal{Y}$ in a given way. To emphasize this point, we write the conformity score function as

$$V(\cdot, \cdot | \hat{\mu}): \mathcal{X} \times \mathcal{Y} \rightarrow \mathbb{R}, \quad (13)$$

such that the role of $\hat{\mu}$ in the score function is fixed. For the ease of presentation, in this subsection, we restrict our attention to binary classification problems with $\mathcal{Y} = \{0, 1\}$ and $c = 0$. The original problem can always be reduced to this setting by a transformation $\tilde{Y} = \mathbb{1}\{Y \leq c\}$.

Recall the preparatory data $\{Z_i\}_{i=1}^{n_1}$, the calibration data $\{Z_i\}_{i=n_1+1}^n$ and the test data $\{\hat{Z}_{n+j}\}_{j=1}^m$ where $\hat{Z}_{n+j} = (X_{n+j}, 0)$. Our goal is to involve all the labeled data $\{Z_i\}_{i=1}^n$ to train an accurate prediction model while still producing a FDR-controlling selection set $\mathcal{S} \subseteq [m]$. Similar to Full Conformal Prediction [Vovk et al., 2005, FCP], the idea of OptCS here is to train the models in a way that is permutation invariant to the calibration data and the j -th test point. Compared with FCP, we only need to plug in the null value $Y_{n+j} = 0$, instead of every hypothesized value $y \in \mathcal{Y}$, which makes the computation easier.

²If \mathcal{A} is a randomized algorithm, this only needs to hold in a distributional sense. Thus, any algorithm can be made symmetric by adding a random permutation of training data before feeding them into the algorithm.

Concretely, for each $\ell \in \{n_1 + 1, \dots, m + n\}$, we train a model $\hat{\mu}_\ell$ using the following as training data:

$$\mathbf{D}_{-\ell} : \{Z_i\}_{i=1}^{n_1} \cup \{Z_i\}_{i=n_1+1}^n \cup \{\hat{Z}_{n+j}\}_{j=1}^m \setminus \tilde{Z}_\ell, \quad (14)$$

where we denote $\tilde{Z}_\ell = Z_\ell$ when $\ell \leq n$ and $\tilde{Z}_\ell = \hat{Z}_\ell$ otherwise. Then, we define the score-generating functional \mathcal{V} via $\mathcal{V}^{(j)} \equiv (V_{n_1+1}, \dots, V_n, \hat{V}_{n+1}, \dots, \hat{V}_{n+m})$, where

$$V_i = V(Z_i | \hat{\mu}_i) \text{ for } i \leq n, \quad \text{and} \quad \hat{V}_{n+j} = V(\hat{Z}_{n+j} | \hat{\mu}_{n+j}) \text{ for } j \in [m]. \quad (15)$$

In other words, for each calibration and test data, we train a prediction model on all data except that specific point, and use the resulting model to compute the conformity score. Note that OptCS-Full needs to train $(n_2 + m)$ many models. While we set $n_1 = 0$ (no split at all) in our experiments, one may increase n_1 to reduce computation complexity at a price of coarsened p-values (the training process still uses all the n labeled data, yet only n_2 samples are used in computing p-values).

Finally, it turns out that applying the BH procedure to the p-values (4) with these scores suffices for FDR control without additional pruning. The following proposition formalizes this idea and guarantees the validity of OptCS-Full, whose proof is in Appendix B.3.

Proposition 4.2. *Suppose the training process of $\hat{\mu}_\ell$ obeys (12). Let \mathcal{S} be the output of Algorithm 1, and \mathcal{S}_{BH} be the output of the BH procedure applied to the p-values (4) with scores (15). Then the followings hold:*

- (i) *The score-generating functional \mathcal{V} in OptCS-Full specified by (15) obeys Definitions 3 and 4.*
- (ii) *Setting $\hat{R}_j \equiv |\mathcal{S}_{\text{BH}}|$ in Algorithm 1 yields $\mathcal{S} = \mathcal{S}_{\text{BH}}$, and \hat{R}_j obeys a relaxed version of Definition 5 that still leads to finite-sample FDR control.*

A caveat of training with the augmented data (14) is that the signal for predicting Y could be diluted by the “null” samples $\{\hat{Z}_{n+j}\}_{j=1}^m$, where the labels are imputed as zero. A remedy we use in our experiments is oversampling to balance the classes in the training process. We discuss another approach in Appendix A.2, which excludes other test points in training the k -th model but increases computation complexity.

We summarize OptCS-Full in Algorithm 2 for clarity as it omits \hat{R}_j and pruning in the general procedure.

Algorithm 2 OptCS-Full

Input: Labeled data $\{(X_i, Y_i)\}_{i=1}^n$, test data $\{X_{n+j}\}_{j=1}^m$, thresholds $\{c_{n+j}\}_{j=1}^m$, FDR target $q \in (0, 1)$, symmetric training algorithm \mathcal{A} .

- 1: (Optional) Split labeled data into preparatory data $\{(X_i, Y_i)\}_{i=1}^{n_1}$ and calibration data $\{(X_i, Y_i)\}_{i=n_1+1}^n$
- 2: **for** $\ell = n_1 + 1, \dots, n + m$ **do**
- 3: Train model $\hat{\mu}_\ell = \mathcal{A}(\{Z_i\}_{i=1}^{n_1} \cup \{\hat{Z}_{n+j}\}_{j=1}^m \setminus \tilde{Z}_\ell)$. // leave-one-out training
- 4: Compute $V_i = V(X_i, Y_i | \hat{\mu}_i)$ for $n_1 < i \leq n$ and $\hat{V}_{n+j} = V(X_{n+j}, c_{n+j} | \hat{\mu}_{n+j})$ for $j \in [m]$.
- 5: **end for**
- 6: **for** $j = 1, \dots, m$ **do**
- 7: Compute p-value p_j via (4) with $V_i^{(j)} \equiv V_i$ for $i = n_1 + 1, \dots, n$, and $\hat{V}_{n+\ell}^{(j)} \equiv \hat{V}_{n+\ell}$ for $\ell \in [m]$.
- 8: **end for**
- 9: Compute selection set \mathcal{S} by applying the BH procedure to $\{p_j\}$ at level q . // no pruning

Output: Selection set \mathcal{S} .

4.3 OptCS-Full-MSel: Model training and selection without data splitting

In this part, we combine the preceding two ideas to propose OptCS-Full-Msel, a variant of Algorithm 1 that allows model training, selection, and FDR-controlling conformal selection with all labeled data. It aims to construct the most powerful test statistic by both leveraging all labeled data and selecting the best model.

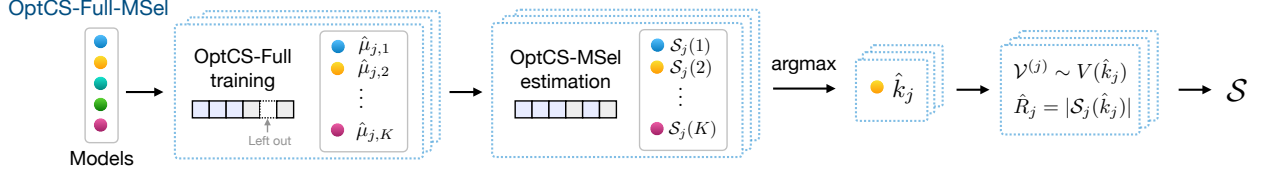


Figure 5: OptCS-Full-MSel uses all labeled data for model training (with ideas similar to OptCS-Full), model selection (with ideas similar to OptCS-MSel), and final multiple testing with selected models.

Since model training is involved, we follow Section 4.2 and assume there are K training processes $\{\mathcal{A}_k\}$ obeying the symmetry condition (12) which lead to K candidate score functions given a set of training data. We encapsulate the functional dependence of each conformity score function on fitted models by writing

$$V(\cdot, \cdot | \hat{\mu}_k, k): \mathcal{X} \times \mathcal{Y} \rightarrow \mathbb{R},$$

where $k \in [K]$ is the model index, and $\hat{\mu}_k$ is any trained model the k -th conformity score function relies on. With slight abuse of notation, here $\hat{\mu}_k$ may also represent general models other than a point predictor (e.g., quantile/mean regression, conditional c.d.f. models). Figure 5 visualizes the pipeline of OptCS-Full-MSel.

The score-generating function \mathcal{V} in OptCS-Full-MSel is specified by

$$\mathcal{V}^{(j)} = (V_{n_1+1}(\hat{k}_j), \dots, V_n(\hat{k}_j), \hat{V}_{n+1}(\hat{k}_j), \dots, \hat{V}_{n+m}(\hat{k}_j)), \quad (16)$$

where $\hat{k}_j \in [K]$ is a selected model constructed similar to OptCS-MSel, and $\{V_i(k)\}_{k=1}^K$ are the scores with the k -th model, obtained from a leave-one-out training process similar to OptCS-Full.

Specifically, we recall the leave-one-out training set $\mathbf{D}_{-\ell}$ in (14) for all $\ell = n_1 + 1, \dots, n + m$, and define

$$V_i(k) = V(X_i, Y_i | \hat{\mu}_{i,k}, k), \quad \hat{V}_{n+j}(k) = V(X_{n+j}, 0 | \hat{\mu}_{n+j,k}, k), \quad \text{where } \hat{\mu}_{\ell,k} = \mathcal{A}_k(\mathbf{D}_{-\ell}). \quad (17)$$

We still distinguish the first n_1 preparatory data and the next n_2 calibration data: while all of them are used in training the model, only the calibration data are involved in the leave-one-out set and the construction of p-values. Similar to OptCS-Full, this preserves the possibility of $n_1 > 0$ to reduce the computation efforts.

Next, we use an idea similar to OptCS-MSel to estimate the selection performance of the k -th model and select the optimal indices $\{\hat{k}_j\}$. With scores computed as (17), for each $j \in [m]$, we set $\mathcal{S}_j(k)$ as the output of the BH procedure applied to $\{\tilde{p}_\ell^{(j)}(k)\}_{\ell \neq j} \cup \{0\}$, where we define the auxiliary p-values

$$\tilde{p}_\ell^{(j)}(k) = \frac{\mathbb{1}\{\hat{V}_{n+j}(k) \leq \hat{V}_{n+\ell}(k)\} + \sum_{i=n_1+1}^n \mathbb{1}\{V_i(k) \leq \hat{V}_{n+\ell}(k)\}}{n_2 + 1}, \quad \ell \neq j.$$

Finally, with $\{\hat{k}_j\}$ and $\{\mathcal{S}_j(k)\}$ in hand, we complete the definition of score generating function \mathcal{V} in (16) (Line 3 of Algorithm 1) and auxiliary selection function \mathcal{R} (Line 5 of Algorithm 1) for OptCS-Full-MSel via

$$\hat{k}_j = \operatorname{argmax}_{k \in [K]} |\mathcal{S}_j(k)|, \quad \hat{\mathcal{R}}_j = |\mathcal{S}_j(\hat{k}_j)|. \quad (18)$$

The next proposition guarantees the validity of OptCS-Full-MSel, whose proof is in Appendix B.4.

Proposition 4.3. *Suppose \mathcal{A}_k obeys the symmetry condition (12) for all $k \in [K]$. Then, the score-generating functional \mathcal{V} in OptCS-Full-MSel specified by (16) obeys Definitions 3 and 4, and the auxiliary selection function \mathcal{R} specified by (18) obeys Definition 5. Therefore, the output of OptCS-Full-MSel obeys $\text{FDR} \leq q$.*

5 Simulation studies

5.1 Conformity score selection with pre-trained models

We first evaluate the performance of OptCS-MSel in the task of selecting conformity scores while producing FDR-controlled selection sets. We treat the set of candidate scores as given before “seeing” the calibration and test data, i.e., the latter two are not involved in the training process. All of the competing methods are:

- (i). **Greedy**: Select the candidate conformity score function which leads to the largest selection set in SCS.
- (ii). **OptCS-MSel_homo** and **OptCS-MSel_hete**: Our method with homogeneous and heterogeneous pruning.
- (iii). **Base_random**: Randomly pick a conformity score and use it in SCS .
- (iv). **Base_cal_split**: Randomly split the calibration set into three folds: $\mathcal{D}_{\text{calib_sel}}$ (25%), $\mathcal{D}_{\text{test_sel}}$ (25%), and $\mathcal{D}'_{\text{calib}}$ (50%). We select the score which leads to the largest selection set in SCS with $\mathcal{D}_{\text{calib_sel}}$ as the calibration set and $\mathcal{D}_{\text{test_sel}}$ as the test set. We then run SCS with calibration set $\mathcal{D}'_{\text{calib}}$.
- (v). **Base_tr_split**: Similar to (iv), but we split $\mathcal{D}_{\text{train}}$ into $\mathcal{D}_{\text{calib_sel}}$ (25%), $\mathcal{D}_{\text{test_sel}}$ (25%), and $\mathcal{D}'_{\text{train}}$ (50%). After training models on $\mathcal{D}'_{\text{train}}$, we use $\mathcal{D}_{\text{calib_sel}}$ (25%), $\mathcal{D}_{\text{test_sel}}$ (25%) to select a score.

We exclude OptCS with deterministic pruning in result reporting since its power is often lower than the other two pruning options, consistent with [Jin and Candès \[2023b\]](#).

Simulation settings. We construct 8 data generating processes, four adapted from [Liang et al. \[2024a\]](#), referred to as Liang’s settings, and four adapted from [Jin and Candès \[2023c\]](#), referred to as Jin’s settings. In all settings, the goal is to identify individuals whose unobserved responses exceed $c_{n+j} \equiv 0$. We design 11 model choices for Liang’s settings and 24 model choices for Jin’s settings. In Liang’s settings, the model quality mostly depends on whether it includes certain features in regression modeling, hence the quality gap between candidate models is large. In Jin’s settings, the model qualities are closer to each other. The detailed data generating processes and model choices are summarized in [Appendix C.1](#). In the experiments, we fix the sample sizes at $n_1 = n_2 = m = 100$ and vary the nominal FDR level $q \in \{0.2, 0.25, \dots, 0.45, 0.5\}$.

Simulation results. We report the empirical FDR and power over $N = 500$ independent runs for Liang’s settings in [Figure 6](#) and for Jin’s settings in [Figure 7](#), with $|\mathcal{D}_{\text{train}}| = 100$, $|\mathcal{D}_{\text{calib}}| = 100$, and $|\mathcal{D}_{\text{test}}| = 100$. The empirical FDR is the mean of $|\mathcal{S} \cap \mathcal{H}_0| / (1 \vee |\mathcal{S}|)$, and the empirical power is the mean of $|\mathcal{S} \cap \mathcal{H}_1| / |\mathcal{H}_1|$ over all replica, where we define $\mathcal{H}_0 = \{j \in [m]: Y_{n+j} \leq c\}$ and $\mathcal{H}_1 = \{j \in [m]: Y_{n+j} > c\}$.

We observe drastic violation of FDR with the **Greedy** method due to the double-dipping bias. In contrast, all other methods control the FDR below the nominal levels. For all 8 settings and across all nominal FDR levels, **OptCS-MSel_homo** consistently outperforms all competing methods that maintain valid FDR control. **OptCS-MSel_hete** outperforms baselines in Liang’s settings. On the other hand, in Jin’s settings with larger nominal FDR levels, model qualities are similar since the random baseline outperforms other baseline methods; in such cases, **OptCS-MSel_homo** maintains strong performance with higher power than **OptCS-MSel_hete**; we conjecture that the smoothing effect of homogeneous pruning is particularly useful.

Finally, we include additional results in [Appendix C.2](#) for the performance of these methods as (n_1, n_2) varies, demonstrating consistent superior performance of OptCS-MSel over baselines.

5.2 Conformal selection without data splitting

Next, we evaluate OptCS-Full described in [Section 4.2](#) and compare it against baseline methods that involves data splits in settings with a fixed model class. Below, we outline all of the competing methods:

- (i). **OptCS-Full_os**: Our procedure in [Algorithm 2](#) with over-sampling in training.
- (ii). **OptCS-Full_sep**: The second variant we introduce in [Appendix A.2](#) that avoids involving all null test samples in training but with more times of model training and additional pruning.
- (iii). **Base_split_0.75**: Randomly split the labeled data into $\mathcal{D}_{\text{train}}$ (75%) and $\mathcal{D}_{\text{calib}}$ (25%). We train the model on $\mathcal{D}_{\text{train}}$, and apply SCS using $\mathcal{D}_{\text{calib}}$ as calibration data.

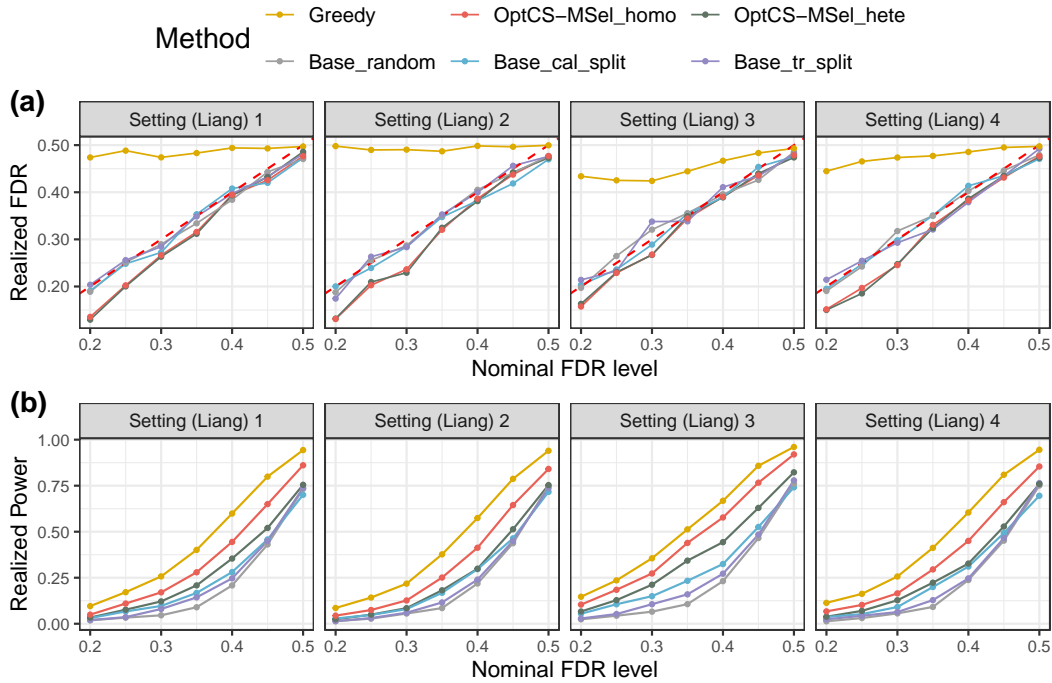


Figure 6: Realized FDR (a) and power (b) for varying nominal FDR levels under Liang’s settings for conformity score selection. Each row corresponds to one data generating process. In these settings, there are significant differences between the selection power with individual conformity scores.

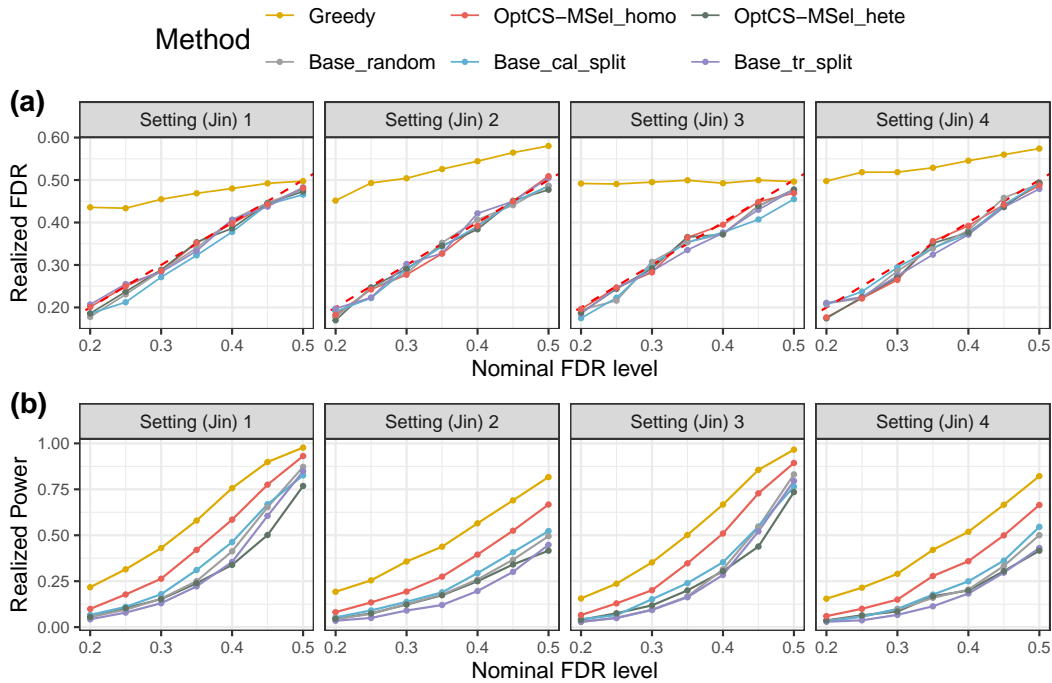


Figure 7: Realized FDR (a) and power (b) for varying nominal FDR levels under Jin’s settings. Each subplot corresponds to one data generating process. In these setting, the selection power with each individual conformity score is similar to each other.

- (iv). `Base_split_0.50`: Similar to (iii), but the data split is $\mathcal{D}_{\text{train}}$ (50%) and $\mathcal{D}_{\text{calib}}$ (50%).
- (v). `Base_split_0.25`: Similar to (iii), but the data split is $\mathcal{D}_{\text{train}}$ (25%) and $\mathcal{D}_{\text{calib}}$ (75%).

Simulation settings. Since Liang’s settings are tailored for the model selection setting (i.e., the performance depends more heavily on regression modeling than training sample size), we exclude them from this experiment. We adapt the four Jin’s settings to classification problems with $Y \in \{0, 1\}$ detailed in Appendix C.3. We fix the sizes of labeled data and test data at $|\mathcal{D}_{\text{label}}| = 500, |\mathcal{D}_{\text{test}}| = 100$. The fixed model choice is $V(x, y) = My - \hat{\mu}(x)$, where $\hat{\mu}: \mathcal{X} \rightarrow [0, 1]$ is fitted by support vector regression (SVR), XGBoost, or Random Forest using the Python library `scikit-learn`, and $M = 100$.

Simulation results. We present the results with the most powerful model, SVR, in Figure 8. Additional results with other two models are in Appendix C.4. In Figure 8, panel (a) shows the tight FDR control of all the methods. Panel (b) shows the superior power of both `OptCS-Full_os` and `OptCS-Full_sep` over SCS baselines with the same amount of labeled data. The most powerful sample splitting scheme in SCS varies with settings, hence in practice it is hard to determine the split ratio when running SCS. In contrast, by utilizing all labeled data in model training, `OptCS-Full` consistently outperforms all of them. Finally, panel (c) shows the power of all competing methods when the total number of labeled data varies. Again, both variants of `OptCS-Full` outperform the baselines across all sample sizes, achieving significant improvement for the most powerful model class.

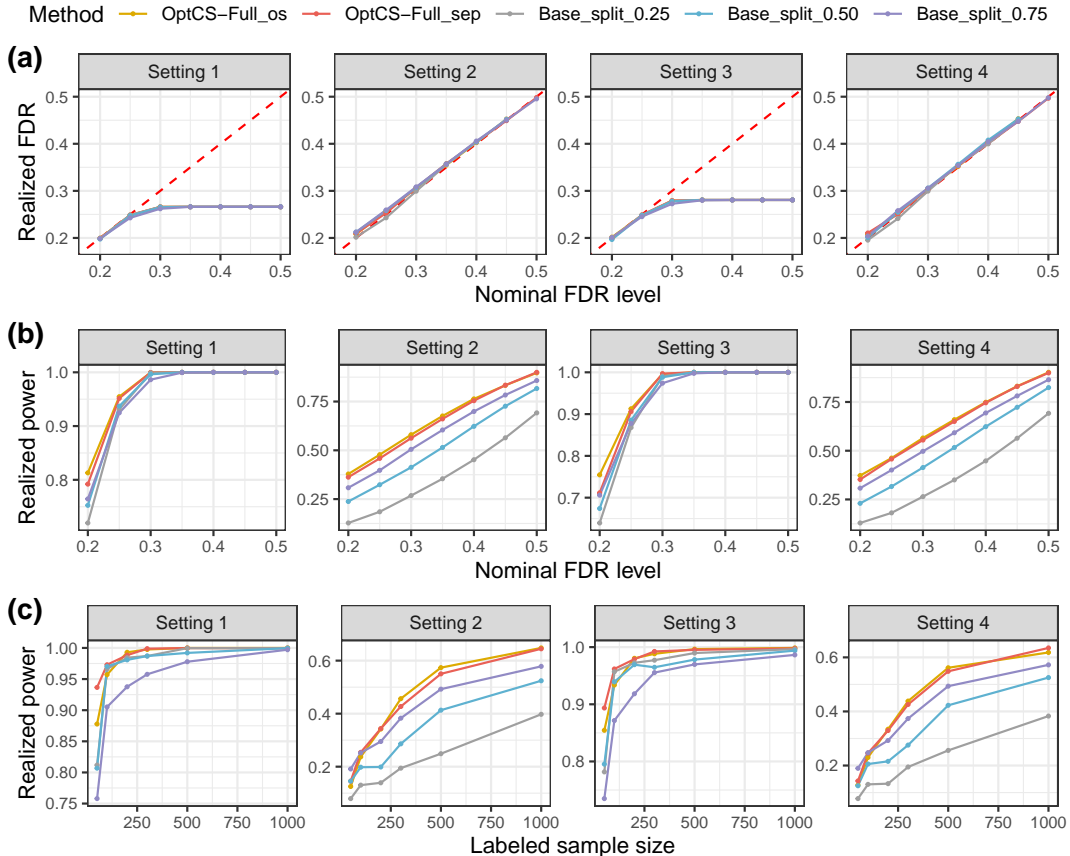


Figure 8: Experiment results for `OptCS-Full` and split conformal selection using SVR as the model class, averaged over $N = 500$ independent runs. **Panel (a)**: Empirical FDR at various nominal FDR levels with $n = 500, m = 100$. **Panel (b)**: Empirical power at various nominal FDR levels with $n = 500, m = 100$. **Panel (c)**: Empirical power with various sizes of labeled samples at fixed nominal FDR level $q = 0.3$.

5.3 Model training and selection with full data

Finally, we conduct simulation studies to demonstrate the performance of OptCS-Full-MSel, which uses all labeled data in the entire process, including model training, model selection, and final multiple testing.

We compare OptCS-Full-MSel with a suite of sample splitting baselines with no techniques from OptCS. These competing methods include:

- (i). **OptCS-Full-MSel**: Our OptCS-Full-MSel procedure where the training process uses over-sampling.
- (ii). **Base_random_0.25**: Randomly split the labeled data into $\mathcal{D}_{\text{train}}$ (25%) and $\mathcal{D}_{\text{calib}}$ (75%). We randomly select a model, train the model on $\mathcal{D}_{\text{train}}$, and apply SCS using $\mathcal{D}_{\text{calib}}$ as calibration data.
- (iii). **Base_random_0.75**: Similar to (ii), but with $\mathcal{D}_{\text{train}}$ (75%) and $\mathcal{D}_{\text{calib}}$ (25%).
- (iv). **Base_split_112**: Randomly split the labeled data into $\mathcal{D}_{\text{train}}$, \mathcal{D}_{sel} , and $\mathcal{D}_{\text{calib}}$ with ratio 1:1:2. We use $\mathcal{D}_{\text{train}}$ to train all the models, use \mathcal{D}_{sel} to run SCS (after additional splitting) and select the model with largest selection set, then use $\mathcal{D}_{\text{calib}}$ to run SCS with the test data and the selected model.
- (v). **Base_split_121**: Similar to (iii), with data split ratio 1:2:1 for $\mathcal{D}_{\text{train}}$, \mathcal{D}_{sel} , and $\mathcal{D}_{\text{calib}}$.
- (vi). **Base_split_211**: Similar to (iii), with data split ratio 2:1:1 for $\mathcal{D}_{\text{train}}$, \mathcal{D}_{sel} , and $\mathcal{D}_{\text{calib}}$.
- (vii). **Base_split_111**: Similar to (iii), with data split ratio 1:1:1 for $\mathcal{D}_{\text{train}}$, \mathcal{D}_{sel} , and $\mathcal{D}_{\text{calib}}$.

To investigate the relative contributions of the full-data training module and the model selection module to the power, we additionally include the following two “partial” baselines in our evaluation:

- (i). **OptCS-Full_random**: Our OptCS-Full procedure where the training process uses over-sampling, with a randomly selected model class (i.e., full-data training but no model selection).
- (ii). **OptCS-Full_split**: We first split the data into \mathcal{D}_{sel} (50%) and $\mathcal{D}_{\text{calib}}$ (50%), then use \mathcal{D}_{sel} to select a model class, and run our OptCS-Full procedure using $\mathcal{D}_{\text{calib}}$ as the “full data” with the selected model class. Inside \mathcal{D}_{sel} , we split the data into a “calibration” fold (50%) and a “test” fold (50%), run OptCS-Full with each model class, and select the one with the largest selection set.

Simulation settings. We adopt the four Jin’s settings adapted from [Jin and Candès, 2023c] and the four Liang’s settings adapted from [Liang et al., 2024a], with 9 model classes for Jin’s settings and 7 model classes for Liang’s settings. We fix the total size of labeled data at $n = 500$ and test data at $m = 100$, and run the experiments for $N = 500$ independent replica. More details on the model setups are in Appendix C.5.

Simulation results. The empirical FDR and power in Liang’s settings are reported in Figure 9. The performance of OptCS-Full with homogeneous and heterogeneous pruning are in red and green solid lines; the two variants both control the FDR. While they yield similar power in Liang’s settings, homogeneous pruning is moderately more powerful in Jin’s settings. Both variants of OptCS-Full consistently outperform all non-OptCS baselines (dashed lines). However, we note that these baselines do not exhaust the FDR budget; this may be due to the fact that the resolution of p-values (determined by calibration data size) is reduced due to sample splitting.

Compared with the two partial baselines (OptCS-Full_split which does not use full sample for model selection and OptCS-Full_random which misses the model selection component), OptCS-Full-MSel demonstrates the benefits of combining the model selection and full-sample training modules. In particular, while the contribution of full-sample training and calibration is significant (comparing OptCS-Full-MSel and OptCS-Full_split), the gap between OptCS-Full-MSel and OptCS-Full_random shows the contribution of model selection seems more significant in Liang’s settings where the quality of models significantly differ.

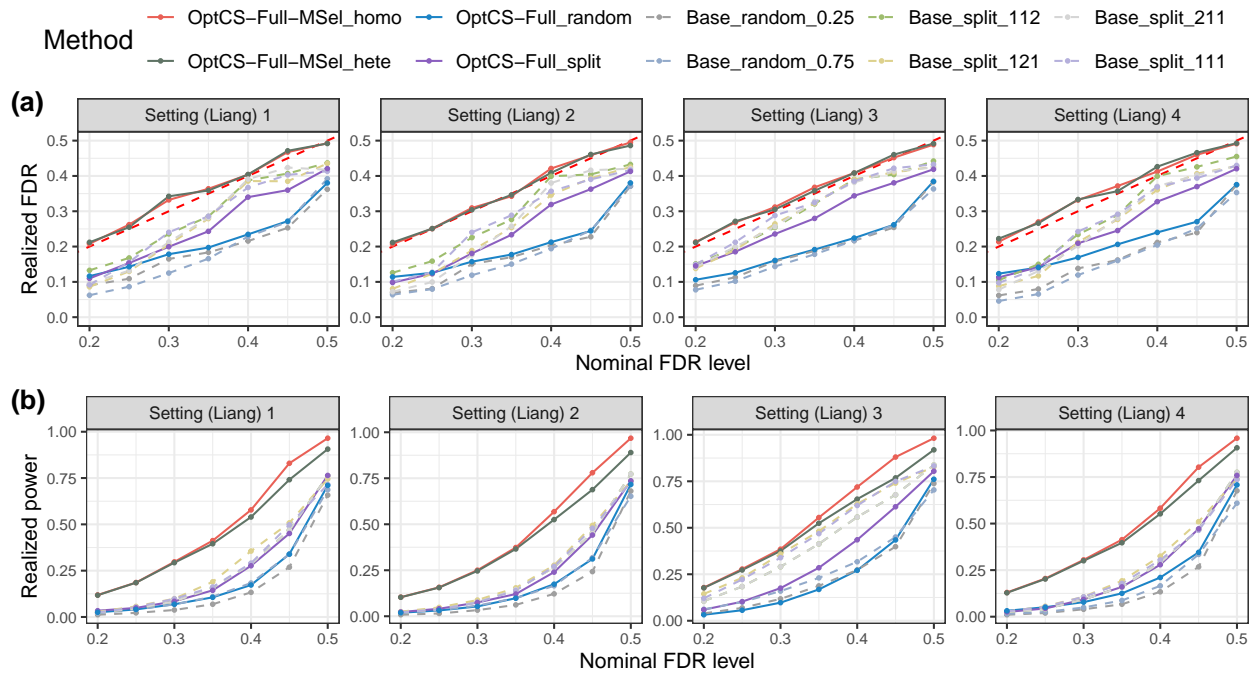


Figure 9: Experiment results for OptCS-Full-MSel and baseline methods in Liang’s settings with $n = 500$ and $m = 100$. **Panel (a)**: Empirical FDR averaged over $N = 500$ independent runs. **Panel (b)**: Empirical power averaged over $N = 500$ independent runs.

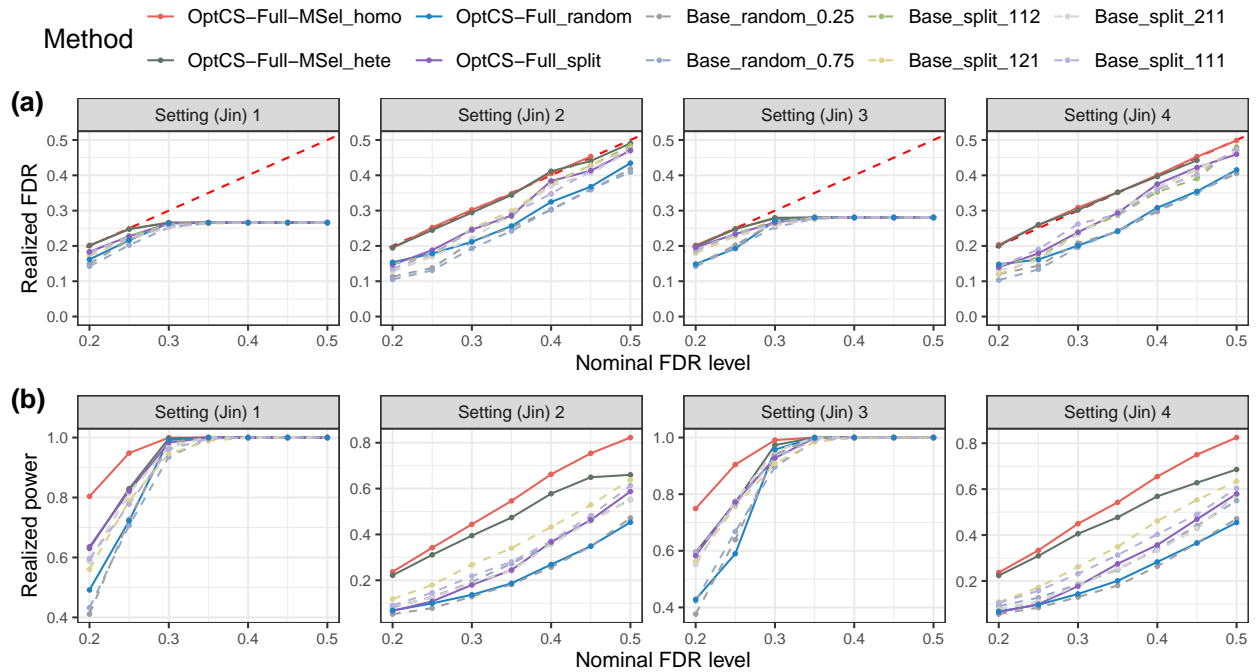


Figure 10: Experiment results for OptCS-Full-MSel and baseline methods in Jin’s settings with $n = 500$ and $m = 100$. Details are otherwise the same as Figure 9.

6 Real data applications

We apply OptCS to two representative applications of Conformal Selection, namely, drug discovery (Section 6.1) and abstention of large language models in radiology report generation (Section 6.2).

6.1 Drug discovery with model selection

We first apply OptCS to drug discovery tasks for selecting drug candidates with favorable biological properties. In this task, controlling the FDR of the selection set ensures that subsequent investigations, such as wet-lab validation of their properties, are resource-efficient.

Concretely, in this problem, each sample is a drug candidate (such as a small molecule, an antibiotic, or a protein), whose physical and chemical features are encoded in $X \in \mathcal{X}$, and we are interested in certain biological property $Y \in \mathcal{Y} \subseteq \mathbb{R}$. While the ground-truth knowledge of Y typically needs to be evaluated via processes such as high-throughput-screening (HTS) or wetlab experiments [Lloyd, Macarron et al., 2011], machine learning models are increasingly used to predict the properties to identify potentially viable candidates before such costly evaluations [Huang, 2007]. Given test drugs $\{X_{n+j}\}_{j=1}^m$, we aim to select promising ones with $Y_{n+j} > c$ for some pre-determined threshold $c > 0$ while controlling the false discovery rate.

For drug property prediction, state-of-the-art models provide a wide variety of pretrained molecule embeddings [Xiong et al., 2019, Li et al., 2021, Landrum, 2016]. These embeddings can be leveraged to train a predictor (e.g., a shallow neural network) in local datasets for a specific downstream task. With the many choices, it is desired to build the selection set with the best model. Among the three procedures, OptCS-MSel is the most suitable for this setting where the models are typically costly to train.

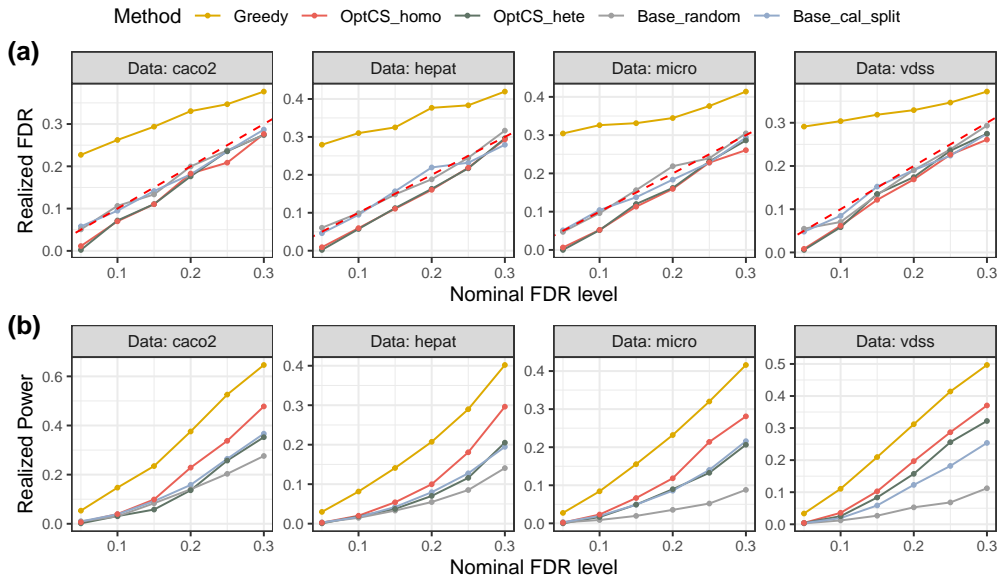


Figure 11: Realized FDR (a) and power (b) for four drug discovery tasks at various nominal FDR levels.

We apply OptCS-MSel to four drug property prediction tasks with data from Therapeutic Data Commons [Huang et al., 2021]. Each dataset is randomly split into training ($\mathcal{D}_{\text{train}}$, 60%), calibration ($\mathcal{D}_{\text{calib}}$, 20%) and test ($\mathcal{D}_{\text{test}}$, 20%) folds. For each dataset, we train 8 prediction models using $\mathcal{D}_{\text{train}}$ from the Deep-Purpose library [Huang et al., 2020], each with one of the following state-of-the-art molecule embeddings: DGL_AttentiveFP, Morgan, CNN, rdkit_2d_normalized, DGL_GCN, DGL_NeuralFP, DGL_GIN_AttrMasking and DGL_GIN_ContextPred. Each prediction model $\hat{\mu}$ is then paired with the standard “clipped” score $M \mathbb{1}\{Y > c\} - \hat{\mu}(x)$ for $M = 1000$, resulting in eight distinct choices. We also fitted nine CNN quantile regression models \hat{q}_α with $\alpha \in \{0.1, 0.2, \dots, 0.9\}$, paired with the clipped quantile score $M \mathbb{1}\{Y > c\} - \hat{q}_\alpha$, $M = 1000$. Here,

the selection threshold c is dataset-dependent: we take it as the 0.7-th quantile of all the labels in the data, such that approximately 30% of the molecules are desirable, i.e. having activity level Y exceeding c .

Figure 11 presents the performance of five methods in Section 5.1 (except `Base_tr_split` which is infeasible using entirely pre-trained models) over $N = 500$ independent runs. We observe similar patterns as in the simulations. While `Greedy` drastically violates the FDR, our methods consistently outperform competing FDR-controlling methods. This shows the ability of OptCS to effectively select powerful pre-trained models to improve the number of discovered promising drug candidates while rigorously controlling the FDR.

6.2 Boosting LLM Alignment

Finally, we study the application of OptCS to aligning large language models for radiology report generation. Following Gui et al. [2024], we use conformal selection to identify radiology images for which the LLM-generated reports meet certain alignment criterion. In this context, FDR control implies that on average, a prescribed fraction (such as 90%) of the selected images indeed have high-quality machine-generated reports, and these selected reports can be deployed in medical decision making with sufficiently low error rate.

Concretely, in this problem, each sample is a “prompt” $X \in \mathcal{X}$, e.g., a radiology image. A vision-to-language model $f \in \mathcal{X} \rightarrow \mathcal{L}$ generates a report summarizing the findings from the image, where \mathcal{L} is the space of reports. To address potential factual errors and other biases in $f(X)$, Conformal Alignment [Gui et al., 2024] defines the alignment status via an indicator $Y = \mathcal{A}(f(X), E) \in \{0, 1\}$, where $E \in \mathcal{E}$ is gold-standard reference information (e.g. a report written by human experts), and $\mathcal{A}: \mathcal{L} \times \mathcal{E} \rightarrow \{0, 1\}$ is a user-specified alignment function. With labeled data $\{(X_i, E_i)\}_{i=1}^n$, Conformal Alignment follows SCS to split the data into two folds. With one fold, it trains a predictor $g: \mathcal{X} \rightarrow [0, 1]$ for the alignment status $Y_i = \mathcal{A}(f(X_i), E_i)$ based on features of the prompt and generated outputs. The second fold is used as calibration data in SCS to select new images $\{X_{n+j}\}_{j=1}^m$ with “aligned” reports ($Y_{n+j} > 0$ should a reference report be acquired).

The power of the procedure depends on the choice of the predictor g and the conformity score, all with many options in practice. Given the scarcity of high-quality reference data, effective use of limited labeled data for model optimization is crucial. In this part, we focus on full-sample training variants which are particularly suitable for the lightweight training processes often used for g (such as random forests).

We use a subset of the MIMIC-CXR dataset [Johnson et al., 2019], and the vision-to-language model is the same as that fine-tuned in Gui et al. [2024]; see Appendix C.6 for details on the datasets and language model. Following Gui et al. [2024], we compute a variety of features based on existing methods for (unsupervised) quantification of uncertainty in LLM outputs; details on the features are in Appendix C.7.

6.2.1 Full-sample training with OptCS-Full

We first apply OptCS-Full to utilize all labeled data in training the alignment predictor given a model class. Given the features, we train three classifiers (logistic regression, random forests, and XGBoost), wrapped by the same conformity score $V(x, y) = My - g(x)$ for $M = 1000$. We fix $n_{\text{labeled}} = 500$ and $m = 100$, where 100 labeled data are used to tune the hyper-parameters in the uncertainty measures, and the remaining are used for selection. We compare OptCS-Full (with over-sampling) with SCS (the method in Gui et al. [2024]) with the recommended split into $|\mathcal{D}_{\text{train}}| = 250$ and $|\mathcal{D}_{\text{calib}}| = 150$, each over $N = 500$ runs.

The empirical FDR and power of the two methods with three model classes under various nominal FDR levels are summarized in Figure 12. Both methods control the FDR. For each model class, the benefit of full-sample training is significant, suggesting the utility of OptCS in settings with limited labeled data.

6.2.2 Combining model selection and full-sample training with OptCS-Full-MSel

We then apply OptCS-Full-MSel to maximize power improvement when given many modeling choices of both the alignment predictor and the conformity score.

After computing the features, we design two setups for the experiments with different model choices. In the first setup, we use all of the features to build mean regression and quantile regression models coupled with

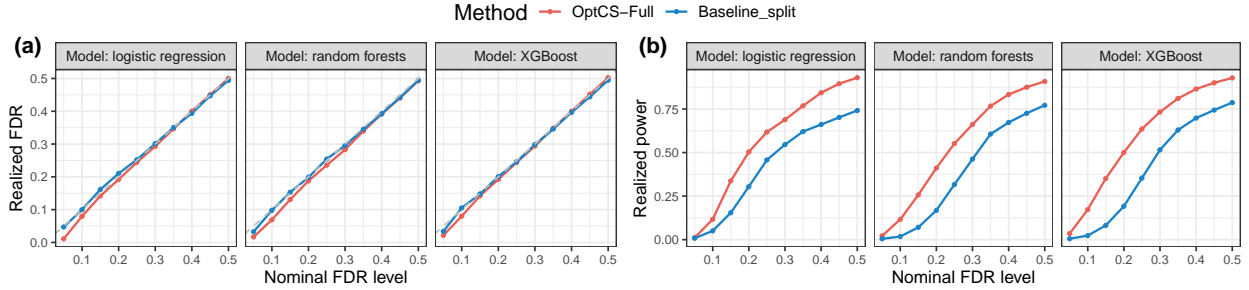


Figure 12: Empirical FDR (a) and power (b) of OptCS-Full and the split baseline for aligning large language models under various nominal FDR levels; results are averaged over $N = 500$ independent runs.

various conformity scores, leading to 12 model choices in total. In the second setup, we vary which features are included in a classifier g trained with the three model classes in Gui et al. [2024], leading to 15 model choices in total. Details for the features, prediction models, and conformity scores are in Appendix C.7. We fix the sample sizes as $n_{\text{labeled}} = 500$ and $m = 100$, using the same data split setup as the preceding part. We compare OptCS-Full-MSel with sample splitting baselines with model selection capabilities similar to those in Section 5.3. The experiments are repeated over $N = 500$ independent runs.

The empirical FDR and power under the two setups are summarized in Figure 13. Due to double-dipping bias, Greedy drastically violates FDR in both setups. For FDR-controlling methods, OptCS-Full outperform the sample splitting baselines, suggesting the power gain from both full-sample training and model selection.

The two setups differ in the gaps between individual model qualities. In the first setup, individual model power differs more significantly, as evident from the advantages of model selection methods over Base_random; in this case, the benefit of model selection is significant. On the other hand, the models qualities are similar in the second setup (while some models only include a subset of features, each subset contains at least a highly informative feature), as evident from Base_random. In this case, the heterogeneous pruning strategy is less powerful, yet the homogeneous pruning remains powerful.

Finally, compared with OptCS-Full in Figure 12, the power gain in OptCS-Full-MSel is reduced because the model classes there are already near-optimal ones, thereby eliminating the difficulty of model selection. Nevertheless, OptCS-Full-MSel still outperforms the split baseline there, indicating its ability to identify the most powerful models as well as power boost from full-sample training.

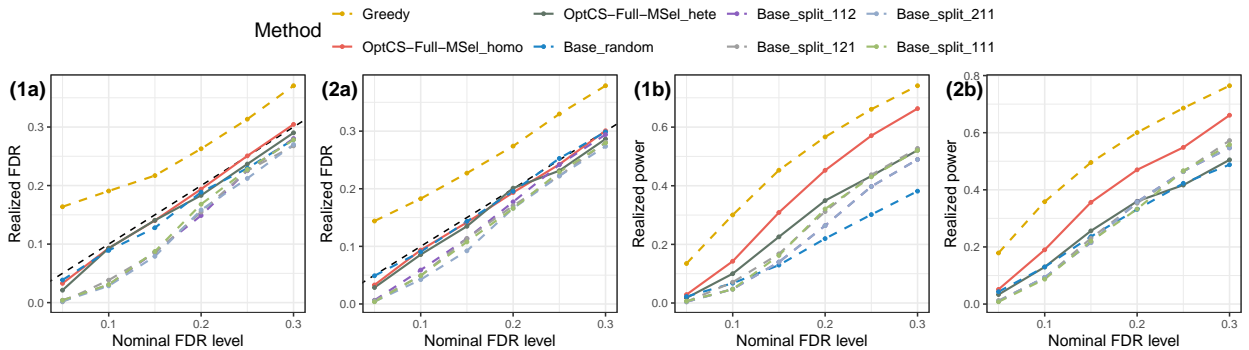


Figure 13: The empirical FDR (Panels (1a) for setup 1 and (2a) for setup 2) and power (Panels (1b) for setup 1 and (2b) for setup 2) of various methods for LLM alignment under various nominal FDR levels.

7 Discussion

In this paper, we propose OptCS, a general framework that allows flexible model optimization in conformal selection. We impose general and mild permutation-based conditions for OptCS to maintain finite-sample, distribution-free FDR control. Under the hood, we propose three concrete procedures, each with distinct model optimization strategies that suit different data and model scenarios. We also use these methods to address the necessity of power improvement via model selection and/or full-sample training in drug discovery and large language model alignment tasks. We conclude the paper with a discussion on potential extensions.

Model optimization strategies may go well beyond selecting from a finite number of candidates and/or full-sample training. For instance, one may aim to optimize an ensemble of several models parameterized via a continuous space. How to develop effective strategies for optimizing over a continuous parameter space with complex objectives (e.g., selection size) remains an important problem, for which ideas from conformal prediction might be useful [Xie et al., 2024, Stutz et al., 2021, Huang et al., 2024].

While we focus on the exchangeable setting here, the needs for model optimization are also present in extensions of conformal selection in more general settings such as covariate shift [Jin and Candès, 2023b] and online selection [Xu and Ramdas, 2024, Huo et al., 2024]. These settings introduce distinct probabilistic structures in data, and hence novel techniques are needed to address data-adaptive model optimization there.

The general technical idea of individualizing the construction of p -values and selection thresholds may extend beyond the model-free selective inference problem to other selective inference problems in conformal inference such as two-sample testing [Hu and Lei, 2024] and outlier detection [Bates et al., 2023]. However, we anticipate that new strategies are needed since the problem structures also differ from here.

References

- Tian Bai, Peng Tang, Yuting Xu, Vladimir Svetnik, Abbas Khalili, Xiang Yu, and Archer Yang. Conformal selection for efficient and accurate compound screening in drug discovery. 2024.
- Stephen Bates, Emmanuel Candès, Lihua Lei, Yaniv Romano, and Matteo Sesia. Testing for outliers with conformal p -values. *The Annals of Statistics*, 51(1):149–178, 2023.
- Yoav Benjamini and Yosef Hochberg. Controlling the false discovery rate: a practical and powerful approach to multiple testing. *Journal of the Royal statistical society: series B (Methodological)*, 57(1):289–300, 1995.
- Yoav Benjamini and Daniel Yekutieli. The control of the false discovery rate in multiple testing under dependency. *The Annals of Statistics*, 29(4):1165 – 1188, 2001. doi: 10.1214/aos/1013699998. URL <https://doi.org/10.1214/aos/1013699998>.
- Paula Carracedo-Reboredo, Jose Liñares-Blanco, Nereida Rodríguez-Fernández, Francisco Cedrón, Francisco J Novoa, Adrian Carballal, Victor Maojo, Alejandro Pazos, and Carlos Fernandez-Lozano. A review on machine learning approaches and trends in drug discovery. *Computational and structural biotechnology journal*, 19:4538–4558, 2021.
- Victor Chernozhukov, Kaspar Wüthrich, and Yinchu Zhu. Distributional conformal prediction. *Proceedings of the National Academy of Sciences*, 118(48):e2107794118, 2021.
- William Fithian and Lihua Lei. Conditional calibration for false discovery rate control under dependence. *The Annals of Statistics*, 50(6):3091–3118, 2022.
- Yu Gui, Ying Jin, and Zhimei Ren. Conformal alignment: Knowing when to trust foundation models with guarantees. *arXiv preprint arXiv:2405.10301*, 2024.
- Pengcheng He, Xiaodong Liu, Jianfeng Gao, and Weizhu Chen. Deberta: Decoding-enhanced bert with disentangled attention. *arXiv preprint arXiv:2006.03654*, 2020.

- Xiaoyu Hu and Jing Lei. A two-sample conditional distribution test using conformal prediction and weighted rank sum. *Journal of the American Statistical Association*, 119(546):1136–1154, 2024.
- Kexin Huang, Tianfan Fu, Lucas M Glass, Marinka Zitnik, Cao Xiao, and Jimeng Sun. Deeppurpose: A deep learning library for drug-target interaction prediction. *Bioinformatics*, 2020.
- Kexin Huang, Tianfan Fu, Wenhao Gao, Yue Zhao, Yusuf Roohani, Jure Leskovec, Connor W Coley, Cao Xiao, Jimeng Sun, and Marinka Zitnik. Therapeutics data commons: Machine learning datasets and tasks for drug discovery and development. *arXiv preprint arXiv:2102.09548*, 2021.
- Kexin Huang, Ying Jin, Emmanuel Candes, and Jure Leskovec. Uncertainty quantification over graph with conformalized graph neural networks. *Advances in Neural Information Processing Systems*, 36, 2024.
- Lei Huang, Weijiang Yu, Weitao Ma, Weihong Zhong, Zhangyin Feng, Haotian Wang, Qianglong Chen, Weihua Peng, Xiaocheng Feng, Bing Qin, et al. A survey on hallucination in large language models: Principles, taxonomy, challenges, and open questions. *arXiv preprint arXiv:2311.05232*, 2023.
- Ziwei Huang. *Drug discovery research: new frontiers in the post-genomic era*. John Wiley & Sons, 2007.
- Yuyang Huo, Lin Lu, Haojie Ren, and Changliang Zou. Real-time selection under general constraints via predictive inference. In *The Thirty-eighth Annual Conference on Neural Information Processing Systems*, 2024.
- Ying Jin and Emmanuel Candès. Model-free selective inference and its applications to drug discovery. In *NeurIPS 2023 Workshop on New Frontiers of AI for Drug Discovery and Development*, 2023a.
- Ying Jin and Emmanuel J Candès. Model-free selective inference under covariate shift via weighted conformal p-values. *arXiv preprint arXiv:2307.09291*, 2023b.
- Ying Jin and Emmanuel J Candès. Selection by prediction with conformal p-values. *Journal of Machine Learning Research*, 24(244):1–41, 2023c.
- Alistair EW Johnson, Tom J Pollard, Seth J Berkowitz, Nathaniel R Greenbaum, Matthew P Lungren, Chih-ying Deng, Roger G Mark, and Steven Horng. MIMIC-CXR, a de-identified publicly available database of chest radiographs with free-text reports. *Scientific data*, 6(1):317, 2019.
- Lorenz Kuhn, Yarin Gal, and Sebastian Farquhar. Semantic uncertainty: Linguistic invariances for uncertainty estimation in natural language generation. *arXiv preprint arXiv:2302.09664*, 2023.
- Greg Landrum. Rdkit: Open-source cheminformatics software. 2016. URL https://github.com/rdkit/rdkit/releases/tag/Release_2016_09_4.
- Jing Lei, Max G'Sell, Alessandro Rinaldo, Ryan J Tibshirani, and Larry Wasserman. Distribution-free predictive inference for regression. *Journal of the American Statistical Association*, 113(523):1094–1111, 2018.
- Mufei Li, Jinjing Zhou, Jiajing Hu, Wenxuan Fan, Yangkang Zhang, Yaxin Gu, and George Karypis. Dgl-lifesci: An open-source toolkit for deep learning on graphs in life science. *ACS Omega*, 2021.
- Ruiting Liang, Wanrong Zhu, and Rina Foygel Barber. Conformal prediction after efficiency-oriented model selection. *arXiv preprint arXiv:2408.07066*, 2024a.
- Ziyi Liang, Matteo Sesia, and Wenguang Sun. Integrative conformal p-values for out-of-distribution testing with labelled outliers. *Journal of the Royal Statistical Society Series B: Statistical Methodology*, page qkad138, 2024b.

- Zhen Lin, Shubhendu Trivedi, and Jimeng Sun. Generating with confidence: Uncertainty quantification for black-box large language models. *arXiv preprint arXiv:2305.19187*, 2023.
- Mathew Lloyd. High-throughput screening as a method for discovering new drugs. URL <https://www.drugtargetreview.com/article/61883/high-throughput-screening-as-a-method-for-discovering-new-drugs/>.
- Ricardo Macarron, Martyn N Banks, Dejan Bojanic, David J Burns, Dragan A Cirovic, Tina Garyantes, Darren VS Green, Robert P Hertzberg, William P Janzen, Jeff W Paslay, et al. Impact of high-throughput screening in biomedical research. *Nature reviews Drug discovery*, 10(3):188–195, 2011.
- Ariane Marandon, Lihua Lei, David Mary, and Etienne Roquain. Adaptive novelty detection with false discovery rate guarantee. *The Annals of Statistics*, 52(1):157–183, 2024.
- Yaniv Romano, Evan Patterson, and Emmanuel Candes. Conformalized quantile regression. *Advances in neural information processing systems*, 32, 2019.
- Yaniv Romano, Matteo Sesia, and Emmanuel Candes. Classification with valid and adaptive coverage. *Advances in Neural Information Processing Systems*, 33:3581–3591, 2020.
- David Stutz, Ali Taylan Cemgil, Arnaud Doucet, et al. Learning optimal conformal classifiers. *arXiv preprint arXiv:2110.09192*, 2021.
- Paweł Szymański, Magdalena Markowicz, and Elżbieta Mikiciuk-Olasik. Adaptation of high-throughput screening in drug discovery—toxicological screening tests. *International journal of molecular sciences*, 13(1):427–452, 2011.
- Vladimir Vovk, Alexander Gammerman, and Glenn Shafer. *Algorithmic learning in a random world*, volume 29. Springer, 2005.
- Xiaoning Wang, Yuyang Huo, Liuhua Peng, and Changliang Zou. Conformalized multiple testing after data-dependent selection. In *The Thirty-eighth Annual Conference on Neural Information Processing Systems*, 2024.
- Laura Weidinger, John Mellor, Maribeth Rauh, Conor Griffin, Jonathan Uesato, Po-Sen Huang, Myra Cheng, Mia Glaese, Borja Balle, Atoosa Kasirzadeh, et al. Ethical and social risks of harm from language models. *arXiv preprint arXiv:2112.04359*, 2021.
- Xiaoyang Wu, Yuyang Huo, Haojie Ren, and Changliang Zou. Optimal subsampling via predictive inference. *Journal of the American Statistical Association*, pages 1–13, 2023.
- Ran Xie, Rina Foygel Barber, and Emmanuel J Candès. Boosted conformal prediction intervals. *arXiv preprint arXiv:2406.07449*, 2024.
- Zhaoping Xiong, Dingyan Wang, Xiaohong Liu, Feisheng Zhong, Xiaozhe Wan, Xutong Li, Zhaojun Li, Xiaomin Luo, Kaixian Chen, Hualiang Jiang, et al. Pushing the boundaries of molecular representation for drug discovery with the graph attention mechanism. *Journal of medicinal chemistry*, 63(16):8749–8760, 2019.
- Ziyu Xu and Aaditya Ramdas. Online multiple testing with e-values. In *International Conference on Artificial Intelligence and Statistics*, pages 3997–4005. PMLR, 2024.
- Yachong Yang and Arun Kumar Kuchibhotla. Selection and aggregation of conformal prediction sets. *Journal of the American Statistical Association*, pages 1–13, 2024.

A Deferred discussion

A.1 Design of auxiliary selection function

In this part, we formalize the discussion in Remark 3.4. For any p-values $\{p_j\}$ and auxiliary selection sizes $\{\widehat{R}_j\}$, define the selection set with heterogeneous, homogeneous, and deterministic pruning as

$$\begin{aligned}\mathcal{S}_{\text{hete}} &= \{j: p_j \leq s_j, \xi_j \widehat{R}_j \leq r_{\text{hete}}^*\}, \quad r_{\text{hete}}^* := \max \left\{ r: \sum_{j=1}^m \mathbb{1} \{p_j \leq s_j, \xi_j \widehat{R}_j \leq r\} \geq r \right\}, \quad \xi_j \stackrel{\text{i.i.d.}}{\sim} \text{Unif}([0, 1]), \\ \mathcal{S}_{\text{homo}} &= \{j: p_j \leq s_j, \xi \widehat{R}_j \leq r_{\text{homo}}^*\}, \quad r_{\text{homo}}^* := \max \left\{ r: \sum_{j=1}^m \mathbb{1} \{p_j \leq s_j, \xi \widehat{R}_j \leq r\} \geq r \right\}, \quad \xi \sim \text{Unif}([0, 1]), \\ \mathcal{S}_{\text{dtm}} &= \{j: p_j \leq s_j, \widehat{R}_j \leq r_{\text{dtm}}^*\}, \quad r_{\text{dtm}}^* := \max \left\{ r: \sum_{j=1}^m \mathbb{1} \{p_j \leq s_j, \widehat{R}_j \leq r\} \geq r \right\}, \quad s_j = q\widehat{R}_j/m.\end{aligned}$$

Also, define the output of the BH procedure applied to $\{p_j\}$ at level $q \in (0, 1)$:

$$\mathcal{S}_{\text{BH}} = \{j: p_j \leq qr_{\text{BH}}^*/m\}, \quad r_{\text{BH}}^* := \max \left\{ r: \sum_{j=1}^m \mathbb{1} \{p_j \leq qr/m\} \geq r \right\}.$$

The following proposition formalizes Remark 3.4.

Proposition A.1. *For any p-values $\{p_j\}$ and any values $\{\widehat{R}_j\}$, the following statements hold:*

- (i) $\mathcal{S}_{\text{hete}} \subseteq \mathcal{S}_{\text{BH}}$, $\mathcal{S}_{\text{homo}} \subseteq \mathcal{S}_{\text{BH}}$, and $\mathcal{S}_{\text{dtm}} \subseteq \mathcal{S}_{\text{BH}}$.
- (ii) If $\widehat{R}_j \equiv |\mathcal{S}_{\text{BH}}|$, then $\mathcal{S}_{\text{hete}} = \mathcal{S}_{\text{homo}} = \mathcal{S}_{\text{dtm}} = \mathcal{S}_{\text{BH}}$.
- (iii) $\mathcal{S}_{\text{dtm}} \subseteq \mathcal{S}_{\text{hete}}$ and $\mathcal{S}_{\text{dtm}} \subseteq \mathcal{S}_{\text{homo}}$.

Proof of Proposition A.1. Fix any values $\{\lambda_j\} \leq 1$. Given any $\{p_j\}$, $\{\widehat{R}_j\}$, and $s_j = q\widehat{R}_j/m$, we denote

$$\mathcal{S}_1(r; \vec{\lambda}) = \{j \in [m]: p_j \leq s_j, \lambda_j \widehat{R}_j \leq r\} = \left\{ j \in [m]: p_j \leq q\widehat{R}_j/m \text{ and } \lambda_j \cdot q\widehat{R}_j/m \leq qr/m \right\},$$

and

$$\mathcal{S}_2(r) = \{j \in [m]: p_j \leq qr/m\}.$$

Then by definition, it is straightforward that $\mathcal{S}_1(r; \vec{\lambda}) \subseteq \mathcal{S}_2(r)$ for any $r \in \mathbb{N}$ and any $\vec{\lambda} \leq \mathbf{1}_m$. Also, for any $r \leq r'$, it holds that $\mathcal{S}_1(r; \vec{\lambda}) \subseteq \mathcal{S}_1(r'; \vec{\lambda})$ and $\mathcal{S}_2(r) \subseteq \mathcal{S}_2(r')$. Define

$$r_1^*(\vec{\lambda}) = \max \left\{ r \in \mathbb{N}: |\mathcal{S}_1(r; \vec{\lambda})| \geq r \right\}, \quad r_2^* = \max \left\{ r \in \mathbb{N}: |\mathcal{S}_2(r)| \geq r \right\}.$$

Since $|\mathcal{S}_1(r; \vec{\lambda})| \leq |\mathcal{S}_2(r)|$ for any $r \in \mathbb{N}$ and any $\vec{\lambda} \leq \mathbf{1}_m$, we know $r_1^*(\vec{\lambda}) \leq r_2^*$, and thus

$$\mathcal{S}_1(r_1^*(\vec{\lambda}); \vec{\lambda}) \subseteq \mathcal{S}_1(r_2^*) \subseteq \mathcal{S}_2(r_2^*).$$

We first use these facts to prove (i). Note that $\mathcal{S}_{\text{BH}} = \mathcal{S}_2(r_2^*)$, and $\mathcal{S}_{\text{hete}} = \mathcal{S}_1(r_1^*(\vec{\xi}); \vec{\xi})$, where $\vec{\xi} = (\xi_1, \dots, \xi_m)$, which leads to $\mathcal{S}_{\text{hete}} \subseteq \mathcal{S}_{\text{BH}}$. Similarly, the fact that $\mathcal{S}_{\text{homo}} = \mathcal{S}_1(r_1^*(\xi \mathbf{1}_m); \xi \mathbf{1}_m)$ leads to $\mathcal{S}_{\text{homo}} \subseteq \mathcal{S}_{\text{BH}}$, and the fact that $\mathcal{S}_{\text{dtm}} = \mathcal{S}_1(r_1^*(\mathbf{1}_m); \mathbf{1}_m)$ leads to $\mathcal{S}_{\text{dtm}} \subseteq \mathcal{S}_{\text{BH}}$.

We then prove (iii) using similar ideas. Consider any $\vec{\lambda} \leq \vec{\eta}$ meaning that $\lambda_j \leq \eta_j$ for all $j \in [m]$. By the definition of $\mathcal{S}_1(r; \vec{\lambda})$, we know $\mathcal{S}_1(r; \vec{\eta}) \subseteq \mathcal{S}_1(r; \vec{\lambda})$ for any $r \in \mathbb{N}$. Further, by the definition of $r_1^*(\vec{\lambda})$, we have $r_1^*(\vec{\eta}) \leq r_1^*(\vec{\lambda})$, and therefore

$$\mathcal{S}_1(r_1^*(\vec{\eta}); \vec{\eta}) \subseteq \mathcal{S}_1(r_1^*(\vec{\eta}); \vec{\lambda}) \subseteq \mathcal{S}_1(r_1^*(\vec{\lambda}); \vec{\lambda}).$$

Thus, since $\vec{\xi} \leq \mathbf{1}_m$, we know $\mathcal{S}_{\text{hete}} = \mathcal{S}_1(r_1^*(\vec{\xi}); \vec{\xi}) \subseteq \mathcal{S}_1(r_1^*(\mathbf{1}_m); \mathbf{1}_m) = \mathcal{S}_{\text{dtm}}$. Since $\xi \mathbf{1}_m \leq \mathbf{1}_m$, we know $\mathcal{S}_{\text{homo}} = \mathcal{S}_1(r_1^*(\xi \mathbf{1}_m); \xi \mathbf{1}_m) \subseteq \mathcal{S}_1(r_1^*(\mathbf{1}_m); \mathbf{1}_m) = \mathcal{S}_{\text{dtm}}$.

Finally, we prove (ii). Note that $r_2^* \leq |\mathcal{S}_2(r_2^*)|$ by the definition of r_2^* . On the other hand, it must hold that $r_2^* \geq |\mathcal{S}_2(r_2^*)|$, as otherwise $|\mathcal{S}_2(r_2^* + 1)| \geq |\mathcal{S}_2(r_2^*)| \geq r_2^* + 1$, contradicting the definition of r_2^* . These two facts imply that $r_2^* = |\mathcal{S}_2(r_2^*)| = |\mathcal{S}_{\text{BH}}|$. For any $\{\lambda_j\} \leq \mathbf{1}_m$, setting $\widehat{R}_j \equiv r_2^*$ implies that for any $r \geq r_2^*$,

$$\mathcal{S}_1(r; \vec{\lambda}) = \left\{ j \in [m]: p_j \leq qr_2^*/m \text{ and } \lambda_j \cdot qr_2^*/m \leq qr/m \right\} = \left\{ j \in [m]: p_j \leq qr_2^*/m \right\} = \mathcal{S}_2(r_2^*), \quad (19)$$

while $\mathcal{S}_1(r; \vec{\lambda}) \subseteq \mathcal{S}_2(r_2^*)$ for any $r < r_2^*$. This implies $r_1^*(\vec{\lambda}) = r_2^*$ for any $\vec{\lambda} \leq \mathbf{1}_m$. Therefore, using (19) and the definitions of the three selection sets, we have $\mathcal{S}_{\text{homo}} = \mathcal{S}_1(r_2^*, \xi \mathbf{1}_m) = \mathcal{S}_2(r_2^*) = \mathcal{S}_{\text{BH}}$, $\mathcal{S}_{\text{hete}} = \mathcal{S}_1(r_2^*, \vec{\xi}) = \mathcal{S}_2(r_2^*) = \mathcal{S}_{\text{BH}}$, and $\mathcal{S}_{\text{dtm}} = \mathcal{S}_1(r_2^*, \mathbf{1}_m) = \mathcal{S}_2(r_2^*) = \mathcal{S}_{\text{BH}}$. This completes the proof of (ii). \square

A.2 A second variant of OptCS-Full

In this part, we present another variant of OptCS that avoids using too many imputed null samples in the leave-one-out training idea of OptCS-Full. We call this variant OptCS-Full_sep.

Following Section 4.2, we assume a training process \mathcal{A} , and write the conformity score function via

$$V(x, y | \widehat{\mu}): \mathcal{X} \times \mathcal{Y} \rightarrow \mathbb{R},$$

where the functional dependence on a trained model is encapsulated in $\widehat{\mu}$ representing a general model. We introduce the procedure of OptCS-Full-One by specifying the two subroutines in Lines 3 and 5 in Algorithm 1.

First, for each $j \in [m]$, we define the leave-one-out training set (again without splitting the labeled data)

$$\mathbf{D}_{-\ell}^{(j)} = \{Z_i\}_{i=1}^n \cup \{Z_{n+j}\} \setminus \{\widetilde{Z}_\ell\},$$

where $\widetilde{Z}_\ell = Z_\ell$ if $\ell \leq n$ and $\widetilde{Z}_\ell = \widehat{Z}_{n+j}$ if $\ell = n + j$. Then, for each $\ell \in [n] \cup \{n + j\}$, we train a model

$$\widehat{\mu}_\ell^{(j)} = \mathcal{A}(\mathbf{D}_{-\ell}^{(j)})$$

using the leave-one-out data. Note that each $\mathbf{D}_{-\ell}^{(j)}$ contains at most one imputed null data point. We then specify the score generating functional in Line 3 of Algorithm 1 via

$$\begin{aligned} \mathcal{V}^{(j)} &= (V_{n_1+1}^{(j)}, \dots, V_n^{(j)}, \widehat{V}_{n+1}^{(j)}, \dots, \widehat{V}_{n+m}^{(j)}), \\ \text{where } V_i^{(j)} &= V(X_i, Y_i | \widehat{\mu}_i^{(j)}), \quad \widehat{V}_{n+\ell}^{(j)} = V(X_{n+\ell}, Y_{n+\ell} | \widehat{\mu}_{n+j}^{(j)}). \end{aligned}$$

In our experiments, we find that running the BH procedure using p-values (4) based on the above scores always controls the empirical FDR. Therefore, we recommend using such a relaxed procedure for use.

If one aims for rigorous theoretical control of FDR in finite samples, we specify the auxiliary selection function $\mathcal{R}(\cdot)$ in Line 5 of Algorithm 1 as follows. We define the auxiliary p-values

$$\widehat{p}_\ell^{(j)} = \frac{\sum_{i=n_1+1}^n \mathbb{1}\{V_i^{(j)} \leq V(X_{n+\ell}, Y_{n+\ell} | \widehat{\mu}_i^{(j)})\} + \mathbb{1}\{\widehat{V}_{n+j}^{(j)} \leq V(X_{n+\ell}, Y_{n+\ell} | \widehat{\mu}_{n+j}^{(j)})\}}{n_2 + 1},$$

and set \widehat{R}_j as the size of the BH procedure output applied to $\{\widehat{p}_\ell^{(j)}\}_{\ell \neq j} \cup \{0\}$. Similar to the proof ideas of Proposition 4.2, we can show that these definitions obey the properties of $\mathcal{V}(\cdot)$ and $\mathcal{R}(\cdot)$ required for finite-sample FDR control in Theorem 3.2.

B Technical proofs

B.1 Proof of Theorem 3.2

Proof of Theorem 3.2. Fix a $j \in [m]$ that corresponds to a null hypothesis, i.e. $Y_{n+j} \leq c_{n+j}$. When computing the scores as the output of \mathcal{V} , consider substituting the j -th test sample \widehat{Z}_{n+j} with Z_{n+j} which use the true response Y_{n+j} . We denote

$$(\bar{V}_{n_1:n}^{(j)}, \bar{V}_{n+1:n+j-1}^{(j)}, \bar{V}_{n+j}^{(j)}, \bar{V}_{n+j+1:n+m}^{(j)}) := \mathcal{V}^{(j)}(Z_{1:n_1}, Z_{n_1+1:n}, \widehat{Z}_{n+1:n+j-1}, Z_{n+j}, \widehat{Z}_{n+j+1:n+m}).$$

We will compare this new set of scores with (3). Note that these scores are unobservable, and are used only for the purpose of analysis. Since \mathcal{V} is monotone for the null (Definition 3), on the null event that $Y_{n+j} \leq c_{n+j}$, we have

$$\bar{V}_i^{(j)} = V_i^{(j)} \text{ for } i \leq n, \quad \bar{V}_{n+i}^{(j)} = \widehat{V}_{n+i}^{(j)} \text{ for } i \leq m, i \neq j, \quad \text{and} \quad \bar{V}_{n+j}^{(j)} \leq \widehat{V}_{n+j}^{(j)}.$$

We now define the oracle p -value as

$$p_j^* := \frac{1 + \sum_{i=n_1+1}^n \mathbb{1}\{\bar{V}_i^{(j)} \leq \bar{V}_{n+j}^{(j)}\}}{n+1}.$$

By definition, $p_j^* \leq p_j$ on the null event that $Y_{n+j} \leq c_{n+j}$. In the next, we seek to prove the subuniformity of p_j^* by an exchangeability argument, and as a result, p_j will be conservative on the event $\{Y_{n+j} \leq c_{n+j}\}$.

Denote $\mathcal{Z}_j = (Z_{n_1+1}, \dots, Z_n, Z_{n+j})$, and also $[\mathcal{Z}_j] = [Z_{n_1+1}, \dots, Z_n, Z_{n+j}]$ as the unordered set of the calibration data and the j -th test point (with true label). We will show that the set of scores $\{\bar{V}_i^{(j)}\}_{i=n_1+1}^n \cup \{\bar{V}_{n+j}^{(j)}\}$ are exchangeable conditional on $[\mathcal{Z}_j] \cup \{\widehat{Z}_{n+\ell}\}_{\ell \neq j}$. Technically, we are to show that for any values $(v_{n_1+1}, \dots, v_n, v_{n+j})$, and any permutation π of $\{n_1+1, \dots, n, n+j\}$,

$$\begin{aligned} & \mathbb{P}\left(\bar{V}_{n_1+1}^{(j)} = v_{n_1+1}, \dots, \bar{V}_n^{(j)} = v_n, \bar{V}_{n+j}^{(j)} = v_{n+j} \mid [\mathcal{Z}_j] \cup \{\widehat{Z}_{n+\ell}\}_{\ell \neq j}\right) \\ &= \mathbb{P}\left(\bar{V}_{n_1+1}^{(j)} = v_{\pi(n_1+1)}, \dots, \bar{V}_n^{(j)} = v_{\pi(n)}, \bar{V}_{n+j}^{(j)} = v_{\pi(n+j)} \mid [\mathcal{Z}_j] \cup \{\widehat{Z}_{n+\ell}\}_{\ell \neq j}\right), \end{aligned} \quad (20)$$

even though they are produced by a highly data-dependent process. For clarity, we write any realized value of the unordered set $[\mathcal{Z}_j]$ as $[z] = [z_{n_1+1}, \dots, z_n, z_{n+j}]$, any realized value of $\{\widehat{Z}_{n+\ell}\}_{\ell \neq j}$ as \widehat{z}_{-j} , and condition on the event $\{[\mathcal{Z}_j] = [z], \{\widehat{Z}_{n+\ell}\}_{\ell \neq j} = \widehat{z}_{-j}\}$ in what follows.

The permutation equivariance of \mathcal{V} (Definition 4) ensures the collection of output scores are not affected by the ordering of data in \mathcal{Z}_j , and as a result, the unordered set of the scores $\{\{\bar{V}_i^{(j)}\}_{i=n_1+1}^n \cup \{\bar{V}_{n+j}^{(j)}\}\}$ is fully determined by $[\mathcal{Z}_j]$ and $\{\widehat{Z}_{n+\ell}\}_{\ell \neq j}$. Thus, the probabilities on both sides of (20) are nonzero if and only if $[v_{n_1+1}, \dots, v_n, v_{n+j}]$ equals the unordered set of $\mathcal{V}^{(j)}(Z_{n_1+1}, \dots, Z_n, \widehat{Z}_{n+1:n+j-1}, Z_{n+j}, \widehat{Z}_{n+j+1:n+m})$. We thus restrict our attention to this case, and without loss of generality, let

$$(v_{n_1+1}, \dots, v_n, v_{n+j}) = \mathcal{V}^{(j)}(z_1, \dots, z_n, \widehat{z}_{n+1:n+j-1}, z_{n+j}, \widehat{z}_{n+j+1:n+m}).$$

We also assume $(v_{n_1+1}, \dots, v_n, v_{n+j})$ are distinct; otherwise we conceptually add an ordering of them to distinguish two elements of the same value.

Given such an event, the only randomness is only in which value in $[z_1, \dots, z_n, z_{n+j}]$ corresponds to the data points Z_1, \dots, Z_n, Z_{n+j} . Since $(Z_{n_1+1}, \dots, Z_n, Z_{n+j})$ is exchangeable given $\{\widehat{Z}_{n+\ell}\}_{\ell \neq j}$, we know that for any permutation π' of $\{n_1+1, \dots, n, n+j\}$,

$$\mathbb{P}\left(Z_{n_1+1} = z_{\pi'(n_1+1)}, \dots, Z_n = z_{\pi'(n)}, Z_{n+j} = z_{\pi'(n+j)} \mid [\mathcal{Z}_j] = [z], \{\widehat{Z}_{n+\ell}\}_{\ell \neq j} = \widehat{z}_{-j}\right) = \frac{1}{(m+n_2)!}.$$

For any permutation π of $\{n_1 + 1, \dots, n, n + j\}$, due to permutation equivariance in Definition 4,

$$\begin{aligned} & \mathbb{P}\left(\bar{V}_{n_1+1}^{(j)} = v_{\pi(n_1+1)}, \dots, \bar{V}_n^{(j)} = v_{\pi(n)}, \bar{V}_{n+j}^{(j)} = v_{\pi(n+j)} \mid [\mathcal{Z}_j] \cup \{\widehat{Z}_{n+\ell}\}_{\ell \neq j}\right) \\ &= \mathbb{P}\left(Z_{n_1+1} = z_{\pi(n_1+1)}, \dots, Z_n = z_{\pi(n)}, Z_{n+j} = z_{\pi(n+j)} \mid [\mathcal{Z}_j] \cup \{\widehat{Z}_{n+\ell}\}_{\ell \neq j}\right) = \frac{1}{(m+n_2)!}. \end{aligned}$$

This proves (20). Similar to the standard result in conformal inference, (20) implies

$$p_j^* \mid [\mathcal{Z}_j] \cup \{\widehat{Z}_{n+\ell}\}_{\ell \neq j} \sim \text{Unif}(\{1/(n+1), \dots, n/(n+1), 1\}).$$

as p_j^* depends on $[\mathcal{Z}_j] \cup \{\widehat{Z}_{n+\ell}\}_{\ell \neq j}$ only through the scores. In other words, for any $t \in [0, 1]$ that is measurable with respect to $[\mathcal{Z}_j] \cup \{\widehat{Z}_{n+\ell}\}_{\ell \neq j}$, we have

$$\mathbb{P}(p_j^* \leq t \mid [\mathcal{Z}_j] \cup \{\widehat{Z}_{n+\ell}\}_{\ell \neq j}) \leq t. \quad (*)$$

This is the conditional subuniformity of the ‘‘oracle’’ conformal p-value p_j^* .

The proof will now rely on the Lemma 9, which is an application of Lemma C.1 from Jin and Candès [2023b], to bound the FDR for all three pruning methods. We will then show FDR control through a series of inequalities. From the lemma, we have

$$\text{FDR} \leq \sum_{j=1}^m \mathbb{E} \left[\frac{\mathbb{1}\{p_j \leq q\widehat{R}_j/m, Y_{n+j} \leq c_{n+j}\}}{1 \vee \widehat{R}_j} \right],$$

and we bound each summand individually below q/m . For any $j \in [m]$, by the permutation invariance of \mathcal{R} under the j -th null (Definition 5), we have

$$\mathcal{R}_0(Z_{1:n_1}, Z_{n_1+1:n}, \widehat{Z}_{n_1+1:n+j-1}, Z_{n+j}, \widehat{Z}_{n+j+1:n+m})_j =: \bar{R}_j \leq \widehat{R}_j,$$

and that the auxiliary selection size \bar{R}_j is measurable given $[\mathcal{Z}_j] \cup \{\widehat{Z}_{n+\ell}\}_{\ell \neq j}$ since it is permutation invariant. Combined with $p_j^* \leq p_j$, this implies

$$\begin{aligned} \mathbb{E} \left[\frac{\mathbb{1}\{p_j \leq q\widehat{R}_j/m, Y_{n+j} \leq c_{n+j}\}}{1 \vee \widehat{R}_j} \right] &\leq \mathbb{E} \left[\frac{\mathbb{1}\{p_j^* \leq q\widehat{R}_j/m, Y_{n+j} \leq c_{n+j}\}}{1 \vee \bar{R}_j} \right] \\ &\leq \mathbb{E} \left[\frac{\mathbb{1}\{p_j^* \leq q\bar{R}_j/m\}}{1 \vee \bar{R}_j} \right]. \end{aligned} \quad (21)$$

Since $q\bar{R}_j/m$ is measurable given $[\mathcal{Z}_j] \cup \{\widehat{Z}_{n+\ell}\}_{\ell \neq j}$,

$$\begin{aligned} \mathbb{E} \left[\frac{\mathbb{1}\{p_j^* \leq q\bar{R}_j/m\}}{1 \vee \bar{R}_j} \mid [\mathcal{Z}_j] \cup \{\widehat{Z}_{n+\ell}\}_{\ell \neq j} \right] &\leq \frac{\mathbb{P}(p_j^* \leq q\bar{R}_j/m \mid [\mathcal{Z}_j] \cup \{\widehat{Z}_{n+\ell}\}_{\ell \neq j})}{1 \vee \bar{R}_j} \\ &\leq q/m. \end{aligned}$$

Finally, taking the expectation over $[\mathcal{Z}_j] \cup \{\widehat{Z}_{n+\ell}\}_{\ell \neq j}$ completes the proof of Theorem 3.2. \square

B.2 Proof of Proposition 4.1

Proof of Proposition 4.1. We begin by proving that the proposed \widehat{R}_j satisfies Definition 5. Fix any $j \in [m]$, and we specify the j -th output of ‘‘oracle’’ functional \mathcal{R}_0 here as that of \mathcal{R} depicted in Section 4.1 with Z_{n+j} used in place of \widehat{Z}_{n+j} . Put another way, the j -th element of \mathcal{R}_0 , which we denote as \bar{R}_j , is defined by the size of the output of the BH procedure applied to $\{\bar{p}_\ell^{(j)}(k)\}$, the ‘‘oracle’’ counterparts of the modified p-values:

$$\bar{p}_\ell^{(j)}(k) = \frac{\sum_{i \in \mathcal{I}_{\text{calib}}} \mathbb{1}\{V_i(k) \leq \widehat{V}_{n+\ell}(k)\} + \mathbb{1}\{V_{n+j}(k) \leq \widehat{V}_{n+\ell}(k)\}}{n_2 + 1}, \quad \ell \in [m], \ell \neq j.$$

Recall that we use the same definitions of $V_i(k)$ and $\widehat{V}_{n+\ell}(k)$. In the above expression, $V_{n+j}(k)$ is used in place of $\widehat{V}_{n+j}(k)$ compared with the modified p-values in (11). We first show that the ‘‘oracle’’ modified p-values $\{\bar{p}_\ell^{(j)}(k)\}_{\ell \neq j}$ are invariant to any permutation on the calibration and test samples $\mathcal{Z}_j := \{Z_{n_1+1}, \dots, Z_n, Z_{n+j}\}$, for any $k \in [K]$ and $\ell \neq j$. By construction,

$$\begin{aligned} \bar{p}_\ell^{(j)}(k) &= \frac{\sum_{i \in \mathcal{I}_{\text{calib}}} \mathbb{1}\{V_i(k) \leq \widehat{V}_{n+\ell}(k)\} + \mathbb{1}\{V_{n+j}(k) \leq \widehat{V}_{n+\ell}(k)\}}{n_2 + 1} \\ &= \frac{\sum_{i \in \mathcal{I}_{\text{calib}} \cup \{n+j\}} \mathbb{1}\{V_i(k) \leq \widehat{V}_{n+\ell}(k)\}}{n_2 + 1} = \frac{\sum_{z \in \mathcal{Z}_j} \mathbb{1}\{V(z; k) \leq V(X_{n+\ell}, c_{n+\ell}; k)\}}{n_2 + 1} \end{aligned}$$

is invariant of any permutation of \mathcal{Z}_j . Denote $\bar{\mathcal{S}}_j(k)$ as the output of BH with the set of oracle modified p-values. Let \bar{k}_j be the oracle version of \widehat{k}_j , i.e., $\bar{k}_j = \operatorname{argmax}_{k \in [K]} |\bar{\mathcal{S}}_j(k)|$. Since $\bar{\mathcal{S}}_j(k)$ is a deterministic function of the modified p-values, it is also permutation invariant to \mathcal{Z}_j for any k . Hence, \bar{k}_j is also permutation invariant to \mathcal{Z}_j .³ This means the oracle auxiliary selection size $\bar{R}_j = |\bar{\mathcal{S}}_j(\bar{k}_j)|$ will also be permutation invariant, establishing the second condition (6) in Definition 5. We then proceed to prove the condition (5) that \mathcal{R} and \mathcal{R}_0 coincide in the j -th element on the null event. Since we use clipped scores, it holds that $V_{n+j}(k) = \widehat{V}_{n+j}(k)$ on the event $\{y_{n+j} \leq c_{n+j}\}$ for all $k \in [K]$. This further implies $\bar{p}_\ell^{(j)}(k) = \widehat{p}_\ell^{(j)}(k)$ for all $\ell \neq j$ and all $k \in [K]$, and therefore $|\bar{\mathcal{S}}_j(k)| = |\mathcal{S}_j(k)|$ for all $k \in [K]$. As a consequence, for any $y_{n+j} \leq c_{n+j}$, we have $\widehat{k}_j = \bar{k}_j$ and $|\bar{\mathcal{S}}_j(\bar{k}_j)| = |\mathcal{S}_j(\widehat{k}_j)|$, which implies that \widehat{R}_j satisfies the first condition (5) in Definition 5.

We now show the permutation equivariance property (Definition 4) of the score-generating functional \mathcal{V} . We will achieve this by showing the permutation invariance of \widehat{k}_j together with the definition of \mathcal{V} . For notational clarity, here we consider any hypothesized values $z'_{1:n_1}$ for $Z_{1:n_1}$, $z_{1:n_2}$ for $Z_{(n_1+1):n}$, and $z_{(n_2+1):(n_2+m)}$ for $\widehat{Z}_{(n_1+1):(n_2+m)}$. Following our definition of OptCS-MSel, for these hypothesized input values, we can write

$$\begin{aligned} \mathcal{V}^{(j)}(z'_{1:n_1}, z_1, \dots, z_{n_2}, z_{(n_2+1):(n_2+j-1)}, z_{n_2+j}, z_{(n_2+j+1):(n_2+m)}) \\ := \left(V(x_1, y_1; \widehat{k}_j), \dots, V(x_{n_2}, y_{n_2}; \widehat{k}_j), V(x_{n_2+1}, y_{n_2+1}; \widehat{k}_j), \dots, V(x_{n+m}, y_{n+m}; \widehat{k}_j) \right), \end{aligned}$$

where $\widehat{k}_j = \widehat{k}_j(z'_{1:n_1}, z_{1:n_2}, z_{(n_2+1):(n_2+m)})$ is the selected model index for each $j \in [m]$.

Using the same arguments as the preceding part, we can show that the modified p-values $\{\widehat{p}_\ell^{(j)}\}_{\ell \neq j}$, and thus the selected model index \widehat{k}_j , are invariant to any permutation of the calibration data and the j -th test point. That is, for any permutation $\pi: \{n_1 + 1, \dots, n, n + j\} \rightarrow \{n_1 + 1, \dots, n, n + j\}$, it holds that

$$\begin{aligned} \widehat{k}_j(z'_{1:n_1}, z_{\pi(1)}, \dots, z_{\pi(n_2)}, z_{(n_2+1):(n_2+j-1)}, z_{\pi(n_2+j)}, z_{(n_2+j+1):(n_2+m)}) \\ = \widehat{k}_j(z'_{1:n_1}, z_1, \dots, z_{n_2}, z_{(n_2+1):(n_2+j-1)}, z_{n_2+j}, z_{(n_2+j+1):(n_2+m)}). \end{aligned}$$

This implies

$$\begin{aligned} \mathcal{V}^{(j)}(z'_{1:n_1}, z_{\pi(1)}, \dots, z_{\pi(n_2)}, z_{(n_2+1):(n_2+j-1)}, z_{\pi(n_2+j)}, z_{(n_2+j+1):(n_2+m)})_i \\ = V\left(x_{\pi(i)}, y_{\pi(i)}; \widehat{k}_j(z'_{1:n_1}, z_{\pi(1)}, \dots, z_{\pi(n_2)}, z_{(n_2+1):(n_2+j-1)}, z_{\pi(n_2+j)}, z_{(n_2+j+1):(n_2+m)})\right) \\ = V\left(x_{\pi(i)}, y_{\pi(i)}; \widehat{k}_j(z'_{1:n_1}, z_1, \dots, z_{n_2}, z_{(n_2+1):(n_2+j-1)}, z_{n_2+j}, z_{(n_2+j+1):(n_2+m)})\right). \end{aligned}$$

Also, again by the definition of $\mathcal{V}^{(j)}$, we have

$$\mathcal{V}^{(j)}(z'_{1:n_1}, z_1, \dots, z_{n_2}, z_{(n_2+1):(n_2+j-1)}, z_{n_2+j}, z_{(n_2+j+1):(n_2+m)})_{\pi(i)}$$

³A random tie-breaking may be involved here. However, as noted earlier, such randomness will not compromise the validity of our approach given that the random variables $\{U_j\}$ are independent of the data.

$$= V\left(x_{\pi(i)}, y_{\pi(i)}; \widehat{k}_j(z'_{1:n_1}, z_1, \dots, z_{n_2}, z_{(n_2+1):(n_2+j-1)}, z_{n_2+j}, z_{(n_2+j+1):(n_2+m)})\right).$$

Comparing the two equations above proves the permutation equivariance property (Definition 4).

Finally, we prove the monotonicity for the null (Definition 3). For $y_{n+j} \leq c_{n+j}$, with slight abuse of notations we let \widehat{k}_j be the selected model index using c_{n+j} and \bar{k}_j be the selected model index using y_{n+j} , while keeping other parts of the inputs intact. By the definition of $\mathcal{V}^{(j)}$, we have

$$\mathcal{V}^{(j)}(z'_{1:n_1}, z_{1:n_2}, \widehat{z}_{n+1:n+j-1}, \widehat{z}_{n+j}, \widehat{z}_{n+j+1:n+m})_{n_2+j} = V(x_{n+j}, c_{n+j}; \widehat{k}_j)$$

and

$$\mathcal{V}^{(j)}(z'_{1:n_1}, z_{1:n_2}, \widehat{z}_{n+1:n+j-1}, z_{n+j}, \widehat{z}_{n+j+1:n+m})_{n_2+j} = V(x_{n+j}, y_{n+j}; \bar{k}_j).$$

Since we use the clipped score, using similar arguments as before, we have $\widehat{k}_j = \bar{k}_j$ when $y_{n+j} \leq c_{n+j}$. Then since each individual score is monotone, we have $V(x_{n+j}, c_{n+j}; \widehat{k}_j) \geq V(x_{n+j}, y_{n+j}; \widehat{k}_j) = V(x_{n+j}, y_{n+j}; \bar{k}_j)$, that is,

$$\mathcal{V}^{(j)}(z'_{1:n_1}, z_{1:n_2}, \widehat{z}_{n+1:n+j-1}, \widehat{z}_{n+j}, \widehat{z}_{n+j+1:n+m})_{n_2+j} \geq \mathcal{V}^{(j)}(z'_{1:n_1}, z_{1:n_2}, \widehat{z}_{n+1:n+j-1}, z_{n+j}, \widehat{z}_{n+j+1:n+m})_{n_2+j}$$

as desired. In addition, for other entries, since $\widehat{k}_j = \bar{k}_j$, we have

$$\mathcal{V}^{(j)}(z'_{1:n_1}, z_{1:n_2}, \widehat{z}_{n+1:n+\ell-1}, \widehat{z}_{n+\ell}, \widehat{z}_{n+\ell+1:n+m})_{\ell} = \mathcal{V}^{(j)}(z'_{1:n_1}, z_{1:n_2}, \widehat{z}_{n+1:n+\ell-1}, z_{n+\ell}, \widehat{z}_{n+\ell+1:n+m})_{\ell}$$

for any $\ell \neq j$. Therefore, we conclude the proof of Proposition 4.1. \square

B.3 Proof of Proposition 4.2

Proof of Proposition 4.2. Fix $j \in [m]$.

We first show the permutation equivariance of \mathcal{V} (Definition 4) given any input values. For notational clarity, we consider hypothesizes inputs $z'_{1:n_1}$ for $Z_{1:n_1}$, $z_{1:n_2}$ for $Z_{(n_1+1):n}$, and $z_{(n_2+1):(n_2+m)}$ for $\widehat{Z}_{(n_2+1):(n_2+m)}$. By construction of the procedure, for any permutation π of $\{1, \dots, n_2, n_2 + j\}$,

$$\begin{aligned} \mathcal{V}^{(j)}(z'_{1:n_1}, z_{\pi(1:n_2)}, z_{n+1}, \dots, z_{\pi(n+j)}, \dots, z_{n+m})_i &= V\left(x_{\pi(i)}, y_{\pi(i)} \mid \widehat{\mu}_{\pi(i)}\right), \quad \text{and} \\ \mathcal{V}^{(j)}(z'_{1:n_1}, z_{1:n_2}, z_{n+1}, \dots, z_{n+j}, \dots, z_{n+m})_{\pi(i)} &= V\left(x_{\pi(i)}, y_{\pi(i)} \mid \widehat{\mu}'_{\pi(i)}\right). \end{aligned}$$

Here, $\widehat{\mu}_{\pi(i)}$ is trained through the algorithm \mathcal{A} on the dataset

$$(z'_{1:n_1}, z_{\pi(1:n_2)}, z_{n+1}, \dots, z_{\pi(n+j)}, \dots, z_{n+m}) \setminus z_{\pi(i)},$$

while $\widehat{\mu}'_{\pi(i)}$ is trained through \mathcal{A} with the same collection of data but in a different order, i.e.,

$$(z'_{1:n_1}, z_{1:n_2}, z_{n+1}, \dots, z_{n+j}, \dots, z_{n+m}) \setminus z_{\pi(i)}.$$

The symmetry (12) of the training algorithm \mathcal{A} guarantees $\widehat{\mu}_{\pi(i)} = \widehat{\mu}'_{\pi(i)}$, which shows the permutation equivariance of \mathcal{V} (Definition 4) given any input values.

The first condition of monotonicity (Definition 3) directly follows from the monotonicity of candidate scores and the fact that $\widehat{\mu}_i$ is not trained on Z_i for any i . We now formally prove the second condition in Definition 3. To this end, we consider hypothesizes inputs $z'_{1:n_1}$ for $Z_{1:n_1}$, $z_{1:n_2}$ for $Z_{(n_1+1):n}$, $\widehat{z}_{(n_2+1):(n_2+m)}$ for $\widehat{Z}_{(n_2+1):(n_2+m)}$ and z_{n+j} for Z_{n+j} . Overriding the notations above, we let $\widehat{\mu}_i$ be the i -th leave-one-out trained model with inputs $(z'_{1:n_1}, z_{1:n_2}, \widehat{z}_{n+1}, \dots, z_{n+j}, \dots, z_{n+m})$ except the i -th data, and $\widehat{\mu}_i^*$ be the i -th leave-one-out trained model with inputs $(z'_{1:n_1}, z_{1:n_2}, z_{n+1}, \dots, z_{n+j}, \dots, z_{n+m})$ except the i -th data. Note that in the classification setting with $y_i \in \{0, 1\}$ and $c_i \equiv 0$, when $y_{n+j} \leq c_{n+j}$, it simply holds that

$y_{n+j} = c_{n+j} = 0$, i.e., $\widehat{z}_{n+j} = z_{n+j}$. As such, we have $\widehat{\mu}_\ell = \widehat{\mu}_\ell^*$ for all $\ell \neq j$, which proves the second condition in Definition 3. Putting the above two facts together, we prove the statement (i).

The first fact in (ii) is an implication of Proposition A.1. Now, we relax Definition 5 by only requiring the first condition (5) to hold when $p_j \leq q\widehat{R}_j/m$ and $y_{n+j} \leq c_{n+j}$. Such relaxation will not compromise the validity of Theorem 3.2, as (21) in the proof of Theorem 3.2 only requires $\bar{R}_j \leq \widehat{R}_j$ when $p_j \leq q\widehat{R}_j/m$.

In the following, we specify \mathcal{R}_0 by defining the j -th output of \mathcal{R}_0 , which we denote as \bar{R}_j . We define the set of oracle modified p-values $\{\bar{p}_\ell^{(j)}\}_{\ell \neq j}$ similar to the ideas in the proof of Proposition 4.1; that is,

$$\bar{p}_\ell^{(j)} = \frac{\sum_{i \in \mathcal{I}_{\text{calib}}} \mathbb{1}\{V_i^* \leq \widehat{V}_{n+\ell}^*\} + \mathbb{1}\{V_{n+j}^* \leq \widehat{V}_{n+\ell}^*\}}{n_2 + 1}, \quad \ell \in [m], \ell \neq j.$$

Here we define the oracle leave-one-out scores

$$V_i^* = V(X_i, Y_i | \widehat{\mu}_i^*), \quad \widehat{V}_{n+\ell}^* = V(X_{n+\ell}, 0 | \widehat{\mu}_{n+\ell}^*),$$

and $\widehat{\mu}_i^*$ is obtained by applying \mathcal{A} to the data

$$\mathbf{D}_{-\ell}^* := (Z_1, \dots, Z_n, \widehat{Z}_{n+1}, \dots, \widehat{Z}_{n+j-1}, Z_{n+j}, \widehat{Z}_{n+j+1}, \dots, \widehat{Z}_{n+m}) \setminus \widetilde{Z}_\ell^*,$$

with $\widetilde{Z}_\ell^* = Z_\ell$ if $\ell \in \{n_2 + 1, \dots, n, n+j\}$ and \widehat{Z}_ℓ otherwise. That is, these are the counterparts of $\{V_i\}$ and $\{\widehat{V}_{n+j}\}$ scores in OptCS-Full when \widehat{Z}_{n+j} is replaced by Z_{n+j} . We then set \bar{R}_j as the selection size of BH applied to $\{\bar{p}_\ell^{(j)}\}_{\ell \neq j} \cup \{0\}$ at nominal level q . Note that we view the quantities defined above (and those in OptCS-Full) implicitly as functions of hypothesized inputs

$$\begin{aligned} \widehat{\mathcal{Z}}_j &:= (Z_{1:n}, \widehat{Z}_{(n+1):(n+m)}) = \widehat{\mathbf{z}}_j := (z'_{1:n_1}, z_{1:n_2}, \widehat{z}_{(n+1):(n+m)}), \\ \mathcal{Z}_j &:= (Z_{1:n}, \widehat{Z}_{(n+1):(n+j-1)}, Z_{n+j}, \widehat{Z}_{(n+j+1):(n+m)}) = \mathbf{z}_j := (z'_{1:n_1}, z_{1:n_2}, \widehat{z}_{(n+1):(n+j-1)}, z_{n+j}, \widehat{z}_{(n+j+1):(n+m)}). \end{aligned}$$

We now show such \mathcal{R}_0 obeys the relaxed version of Definition 5 we propose. Specifically, we will show that (a) \bar{R}_j is permutation invariant \mathbf{z}_j , and (b) $\bar{R}_j = |\mathcal{S}_{\text{BH}}|$ when $p_j \leq s_j = q\widehat{R}_j/m$ and $y_{n+j} \leq c_{n+j}$.

To show (a), we note each $\bar{p}_\ell^{(j)}$ is invariant to permutations of \mathbf{z}_j . Formally, for any permutation π , we denote the corresponding $\bar{p}_\ell^{(j)}$ with inputs \mathbf{z}_j permuted by π as $\bar{p}_\ell^{(j)}(\pi)$. Then by definition,

$$\bar{p}_\ell^{(j)}(\pi) = \frac{\sum_{i \in \mathcal{I}_{\text{calib}} \cup \{n+j\}} \mathbb{1}\{V_{\pi(i)}^* \leq \widehat{V}_{n+\ell}^*\}}{n_2 + 1} = \bar{p}_\ell^{(j)},$$

where we use the fact that after permutation, the i -th leave-one-out trained model $\widehat{\mu}_i^*$ remains intact due to the symmetry of \mathcal{A} . Since each $\bar{p}_\ell^{(j)}$ is invariant to permutations of $\{Z_{n_1+1}, \dots, Z_n, Z_{n+j}\}$, so is the output of BH applied to them, and so is \bar{R}_j . This proves (a).

We now show the relaxed condition (b). Since in the binary setting with $Y_{n+j} \in \{0, 1\}$ and $c_{n+j} \equiv 0$, we know that on the null event $\{Y_{n+j} \leq c_{n+j}\}$, it holds that $Y_{n+j} = c_{n+j} = 0$ and hence

$$\mathbf{D}_{-\ell}^* = \mathbf{D}_{-\ell}, \quad \widehat{\mu}_i^* = \widehat{\mu}_i, \quad V_i^* = V_i, \quad \widehat{V}_{n+\ell}^* = \widehat{V}_{n+\ell}, \quad \text{and} \quad V_{n+j} = \widehat{V}_{n+j}.$$

That is, $Y_{n+j} \leq c_{n+j}$ implies

$$\bar{p}_\ell^{(j)} = \frac{\sum_{i \in \mathcal{I}_{\text{calib}}} \mathbb{1}\{V_i \leq \widehat{V}_{n+\ell}\} + \mathbb{1}\{\widehat{V}_{n+j} \leq \widehat{V}_{n+\ell}\}}{n_2 + 1} =: p_\ell^{(j)}.$$

That is, \bar{R}_j is the output of BH procedure (at nominal level q) applied to $\{p_\ell^{(j)}\}$ on the null event $\{y_{n+j} \leq c_{n+j}\}$, and $p_\ell^{(j)}$ are in terms of observed inputs. Now assuming $y_{n+j} \leq c_{n+j}$ and $p_j \leq s_j := q\widehat{R}_j/m$, we are to show the relaxed conditions with $p_\ell^{(j)}$ in the place of $\bar{p}_\ell^{(j)}$. We consider the following two cases:

- (i). If $\widehat{V}_{n+j} \leq \widehat{V}_{n+l}$, then $V_{n+j} \leq \widehat{V}_{n+l}$ by the monotonicity of V . In this case we have $\bar{p}_l^{(j)} = p_l \geq p_j$.
- (ii). If $\widehat{V}_{n+j} > \widehat{V}_{n+l}$, then $p_l \leq p_j$; it also holds that

$$p_l^{(j)} \leq \frac{\sum_{i \in \mathcal{I}_{\text{calib}}} \mathbb{1}\{V_i \leq \widehat{V}_{n+l}\} + 1}{n_2 + 1} \leq \frac{\sum_{i \in \mathcal{I}_{\text{calib}}} \mathbb{1}\{V_i \leq \widehat{V}_{n+j}\} + 1}{n_2 + 1} = p_j.$$

That $p_j \leq s_j = q|\mathcal{S}_{\text{BH}}|/m = q|\mathcal{S}_{\text{BH}}|/m$ indicates $j \in \mathcal{S}_{\text{BH}}$, i.e. the j -th test sample is (falsely) rejected. In this case, if we change the set of input p-values to the BH procedure from

$$p_1, \dots, p_{j-1}, p_j, p_{j+1}, \dots, p_m \quad \text{to} \quad p_1^{(j)}, \dots, p_{j-1}^{(j)}, 0, p_{j+1}^{(j)}, \dots, p_m^{(j)},$$

all the p-values larger than p_j will be kept unchanged by (i), and no new rejections can be made as p_j is rejected. In addition, all the p-values $p_l \leq p_j$ will remain no greater than p_j after the replacement by (ii), so the p-value ranked at j must not increase, leading to a rejection set of size at least $|\mathcal{S}_{\text{BH}}| = \widehat{R}_j$. The two facts imply that $\bar{R}_j = \widehat{R}_j$ when $y_{n+j} \leq c_{n+j}$ and $p_j \leq s_j$, demonstrating the first condition and hence the relaxed permutation invariance of \mathcal{R}_0 . We thus conclude the proof of Proposition 4.2. \square

B.4 Proof of Proposition 4.3

Proof of Proposition 4.3. Fix any $j \in [m]$.

We first show the permutation equivariance of the score functional (Definition 4). Namely, we consider \mathcal{V} with any hypothesized inputs $\mathbf{z} = (z'_{1:n_1}, z_{1:n_2+m})$ and any permutation π of $\mathcal{I}_j := \{1, \dots, n_2, n_2 + j\}$. As such, all quantities defined in OptCS-Full-MSel can be implicitly viewed as functions of \mathbf{z} . The permuted input is denoted as $\pi(\mathbf{z}) := (z'_{1:n_1}, z_{\pi(n_1+1:n)}, z_{n+1}, \dots, z_{\pi(n+j)}, \dots, z_{n+m})$.

Similar to the proof of Proposition 4.2, since each \mathcal{A}_k is symmetric to the inputs, each trained model $\widehat{\mu}_{i,k}$ is invariant to permutations of $(z_1, \dots, z_{n_2}, z_{n_2+j})$. Denote $\widehat{\mu}_{i,k}^\pi$ as the model trained via \mathcal{A}_k by leaving out the i -th element with the permuted inputs $\pi(\mathbf{z})$. Due to the symmetry of \mathcal{A}_k , we have

$$\widehat{\mu}_{i,k}^\pi = \widehat{\mu}_{i,k}.$$

Denote the modified p-values $p_\ell^{(j)}(k)$ obtained after the permutation π as $p_\ell^{(j)}(k, \pi)$. This implies

$$\begin{aligned} p_\ell^{(j)}(k, \pi) &= \frac{\sum_{i \in \mathcal{I}_j} \mathbb{1}\{V(x_{\pi(i)}, y_{\pi(i)}; \widehat{\mu}_{\pi(i),k}^\pi, k) \leq V(x_{n+l}, y_{n+l}, \widehat{\mu}_{\ell,k}^\pi, k)\}}{n_2 + 1} \\ &= \frac{\sum_{i \in \mathcal{I}_j} \mathbb{1}\{V(x_i, y_{\pi(i)}; \widehat{\mu}_{i,k}, k) \leq V(x_{n+l}, y_{n+l}, \widehat{\mu}_{\ell,k}, k)\}}{n_2 + 1} = \bar{p}_\ell^{(j)}(k). \end{aligned}$$

(Note that for the ℓ -th test point, y_{n+l} is a general hypothesized input which shall be understood as a hypothesized value for the observed threshold c_{n+l}).

That is, all the modified p-values, hence \widehat{k}_j , as a function of the input values, are permutation invariant with respect to $(z_1, \dots, z_{n_2}, z_{n_2+j})$. Therefore, for any permutation π of \mathcal{I}_j , we have

$$\begin{aligned} \mathcal{V}^{(j)}(z'_{1:n_1}, z_{1:n_2+m})_{\pi(i)} &= V(\widetilde{z}_{\pi(i)} | \widehat{\mu}_{\pi(i), \widehat{k}_j}, \widehat{k}_j), \quad \text{and} \\ \mathcal{V}^{(j)}(z'_{1:n_1}, z_{\pi(n_1+1:n)}, z_{n+1}, \dots, z_{\pi(n+j)}, \dots, z_{n+m})_i &= V(\widetilde{z}_{\pi(i)} | \widehat{\mu}_{\pi(i), \widehat{k}_j}, \widehat{k}_j), \end{aligned}$$

where we denote $\widetilde{z}_i = (x_i, y_i)$ if $i \leq n_2$ and $\widetilde{z}_i = (x_i, c_i)$ otherwise. This proves Definition 4.

We then show the monotonicity property in Definition 3. Overriding the notations a bit, we consider any hypothesized inputs $\widehat{\mathbf{z}} := (z'_{1:n_1}, z_{1:n_2}, \widehat{z}_{n+1:n+m})$ and $\widehat{\mathbf{z}} := (z'_{1:n_1}, \widehat{z}_{1:n+j-1}, z_{n+j}, \widehat{z}_{(n+j+1):(n+m)})$, with $\widehat{z}_{n+j} = (x_{n+j}, c_{n+j})$, $z_{n+j} = (x_{n+j}, c_{n+j})$, and $y_{n+j} \leq c_{n+j}$. In the classification setting with $y_{n+j} \in \{0, 1\}$ and $c_{n+j} = 0$, we know $y_{n+j} \leq c_{n+j}$ implies $y_{n+j} = c_{n+j}$ hence $\widehat{\mathbf{z}} = \mathbf{z}$. As such, the j -th set of score outputs $\mathcal{V}^{(j)}$ remain the same, which proves Definition 3.

We now show that \mathcal{R} satisfies Definition 5. Fix any $j \in [m]$. To compute \mathcal{R}_0 , we will apply the BH procedure at nominal level q to the set of oracle slightly modified p-values:

$$\bar{p}_\ell^{(j)}(k) = \frac{\sum_{i=n_2+1}^n \mathbb{1}\{V_i^*(k) \leq \widehat{V}_{n+\ell}^*(k)\} + \mathbb{1}\{V_{n+j}^*(k) \leq \widehat{V}_{n+\ell}^*(k)\}}{n_2 + 1}, \quad \ell \in [m], \ell \neq j,$$

where $V_i^*(k)$ and $\widehat{V}_{n+\ell}^*(k)$ are the leave-one-out trained scores

$$V_i^*(k) = V(X_i, Y_i | \widehat{\mu}_{i,k}^*, k), \quad \widehat{V}_{n+\ell}^*(k) = V(X_{n+\ell}, 0 | \widehat{\mu}_{n+\ell,k}^*, k),$$

and $\widehat{\mu}_{i,k}^*$ is obtained by applying \mathcal{A}_k to the data

$$\mathbf{D}_{-\ell}^* := (Z_1, \dots, Z_n, \widehat{Z}_{n+1}, \dots, \widehat{Z}_{n+j-1}, Z_{n+j}, \widehat{Z}_{n+j+1}, \dots, \widehat{Z}_{n+m}) \setminus \widetilde{Z}_\ell^*,$$

with $\widetilde{Z}_\ell^* = Z_\ell$ if $\ell \in \{n_2 + 1, \dots, n, n + j\}$ and \widehat{Z}_ℓ otherwise. Similar to the proof of Proposition 4.2, these are oracle scores obtained in the same way as those in OptCS-Full except that \widehat{Z}_{n+j} is replaced by Z_{n+j} . We denote $\bar{\mathcal{S}}_j(k)$ as the output of BH applied to p-values $\{\bar{p}_\ell^{(j)}(k)\}_{\ell \neq j} \cup \{0\}$ at the same nominal level q , and define the oracle selected model index $\bar{k}_j := \operatorname{argmax}_{k \in [K]} |\bar{\mathcal{S}}_j(k)|$.

For conceptual clarity, while we use the current notations, all these quantities are implicitly functions of (hypothesizes) inputs

$$\begin{aligned} \widehat{\mathbf{Z}}_j &:= (Z_{1:n}, \widehat{\mathbf{Z}}_{(n+1):(n+m)}) = \widehat{\mathbf{z}}_j := (z'_{1:n_1}, z_{1:n_2}, \widehat{z}_{(n+1):(n+m)}), \\ \mathcal{Z}_j &:= (Z_{1:n}, \widehat{\mathbf{Z}}_{(n+1):(n+j-1)}, Z_{n+j}, \widehat{\mathbf{Z}}_{(n+j+1):(n+m)}) = \mathbf{z}_j := (z'_{1:n_1}, z_{1:n_2}, \widehat{z}_{(n+1):(n+j-1)}, z_{n+j}, \widehat{z}_{(n+j+1):(n+m)}). \end{aligned}$$

We first show the permutation invariance of such \mathcal{R}_0 . This relies on the fact that $\{\bar{p}_\ell^{(j)}(k)\}_{\ell \neq j}$ are invariant to any permutation on $\mathcal{Z}_j = \{Z_{n_1+1}, \dots, Z_n, Z_{n+j}\}$ for any $k \in [K]$ and $\ell \neq j$. Denoting $\mathcal{I}_{\text{calib}} = \{n_2 + 1, \dots, n\}$, we have

$$\begin{aligned} \bar{p}_\ell^{(j)}(k) &= \frac{\sum_{i \in \mathcal{I}_{\text{calib}}} \mathbb{1}\{V_i^*(k) \leq \widehat{V}_{n+\ell}^*(k)\} + \mathbb{1}\{V_{n+j}^*(k) \leq \widehat{V}_{n+\ell}^*(k)\}}{n_2 + 1} \\ &= \frac{\sum_{i \in \mathcal{I}_{\text{calib}} \cup \{n+j\}} \mathbb{1}\{V_i(k) \leq \widehat{V}_{n+\ell}^*(k)\}}{n_2 + 1}. \end{aligned}$$

By the symmetry of \mathcal{A}_k , we know that $\widehat{V}_{n+\ell}^*(k)$ is invariant to any permutation of $\{Z_{n_1+1}, \dots, Z_n, Z_{n+j}\}$. On the other hand, for each $i \in \mathcal{I}_{\text{calib}} \cup \{n+j\}$, the trained model by leaving this data point out remains the same under permutations of $\{Z_{n_1+1}, \dots, Z_n, Z_{n+j}\}$. Denoting the corresponding $\bar{p}_\ell^{(j)}(k)$ obtained after permutation π as $\bar{p}_\ell^{(j)}(k, \pi)$, we then have

$$\bar{p}_\ell^{(j)}(k, \pi) = \frac{\sum_{i \in \mathcal{I}_{\text{calib}} \cup \{n+j\}} \mathbb{1}\{V_{\pi(i)}(k) \leq \widehat{V}_{n+\ell}^*(k)\}}{n_2 + 1} = \bar{p}_\ell^{(j)}(k).$$

Since BH is a deterministic function of the input p-values, we know that $\bar{\mathcal{S}}_j(k)$ is permutation invariant with respect to $\{Z_{n_1+1}, \dots, Z_n, Z_{n+j}\}$ for any $k \in [K]$, and consequently, \bar{k}_j is also permutation invariant up to a random, independent tie-breaking. This establishes condition (6) in Definition 5 as $\bar{R}_j = |\bar{\mathcal{S}}_j(\bar{k}_j)|$ by construction.

We now show the first condition in Definition 5. Since in the binary setting with $Y_{n+j} \in \{0, 1\}$ and $c_{n+j} \equiv 0$, we know that on the null event $\{Y_{n+j} \leq c_{n+j}\}$, it holds that $Y_{n+j} = c_{n+j} = 0$ and hence

$$\mathbf{D}_{-\ell}^* = \mathbf{D}_{-\ell}, \quad \widehat{\mu}_{i,k}^* = \widehat{\mu}_{i,k}, \quad V_i^*(k) = V_i(k), \quad \widehat{V}_{n+\ell}^*(k) = \widehat{V}_{n+\ell}(k).$$

This implies $\widehat{R}_j = \bar{R}_j$ on the null event, as \widehat{R}_j and \bar{R}_j are obtained by the same procedure to these two sets of scores. We thus conclude that \mathcal{R} obeys Definition 5. \square

B.5 Proof of Lemma 3.3

Proof of Lemma 3.3. We prove the result for three pruning options separately.

Case 1: Homogeneous pruning. By definition, we have

$$\text{FDR} = \mathbb{E} \left[\frac{\sum_{j=1}^m \mathbb{1}\{j \in \mathcal{S}, Y_{n+j} \leq c_{n+j}\}}{1 \vee |\mathcal{S}|} \right] = \mathbb{E} \left[\frac{\sum_{j=1}^m \mathbb{1}\{p_j \leq s_j, Y_{n+j} \leq c_{n+j}\} \mathbb{1}\{\xi_j \leq |\mathcal{S}|/\widehat{R}_j\}}{1 \vee |\mathcal{S}|} \right]$$

where the second inequality relies on that $r^* = |\mathcal{S}|$, a property that follows from the proof of Proposition A.1. Fix any $j \in [m]$. Once $j \in \mathcal{S}$, the rejection set of our pruning method will not change if ξ_j is sent to 0 while keeping other ξ 's unchanged, by the step-up nature of the pruning process. Denoting $\mathcal{S}_{\xi_j \rightarrow 0}$ as the rejection set obtained by replacing ξ_j by 0 in the pruning step, we have

$$\begin{aligned} \text{FDR} &= \sum_{j=1}^m \sum_{k=1}^m \mathbb{E} \left[\frac{\mathbb{1}\{|\mathcal{S}| = k\}}{k} \mathbb{1}\{p_j \leq s_j, Y_{n+j} \leq c_{n+j}\} \mathbb{1}\{\xi_j \leq k/\widehat{R}_j\} \right] \\ &\leq \sum_{j=1}^m \sum_{k=1}^m \mathbb{E} \left[\frac{\mathbb{1}\{|\mathcal{S}_{\xi_j \rightarrow 0}| = k\}}{k} \mathbb{1}\{p_j \leq s_j, Y_{n+j} \leq c_{n+j}\} \mathbb{1}\{\xi_j \leq k/\widehat{R}_j\} \right] \\ &= \sum_{j=1}^m \sum_{k=1}^m \mathbb{E} \left[\frac{\mathbb{1}\{|\mathcal{S}_{\xi_j \rightarrow 0}| = k\}}{\widehat{R}_j} \mathbb{1}\{p_j \leq s_j, Y_{n+j} \leq c_{n+j}\} \right] = \sum_{j=1}^m \mathbb{E} \left[\frac{\mathbb{1}\{p_j \leq s_j, Y_{n+j} \leq c_{n+j}\}}{\widehat{R}_j} \right] \end{aligned}$$

where the second equality follows from the independence between ξ_j and $(\mathcal{S}_{\xi_j \rightarrow 0}, p_j, \widehat{R}_j)$. This shows the homogeneous case.

Case 2: Heterogeneous pruning. In this case, we use a conditional PRDS property of $\{\xi \widehat{R}_j\}_{j=1}^m$ which we will specify later. Let $\mathbb{E}_{\mathcal{D}}$ be the conditional expectation given all the data, so the only randomness lies in ξ . By the independence of ξ , we would still have $\xi \sim \text{Unif}([0, 1])$ after conditioning. We define the conditional FDR:

$$\text{FDR}(\mathcal{D}) := \mathbb{E}_{\mathcal{D}} \left[\frac{\sum_{j=1}^m \mathbb{1}\{j \in \mathcal{S}, Y_{n+j} \leq c_{n+j}\}}{1 \vee |\mathcal{S}|} \right]$$

where $\mathbb{E}_{\mathcal{D}}$ is with respect to the randomness in ξ conditional on $\mathcal{D} := \mathcal{D}_{\text{label}} \cup \{(X_{n+j}, c_{n+j})\}_{j=1}^m$. Note that $\mathbb{1}\{p_j \leq s_j\}$ are deterministic conditional on the data. We denote $\mathcal{S}^{(1)} := \{j : p_j \leq s_j\}$ as the first-step rejection set, and $\mathcal{H}_0 := \{j : Y_{n+j} \leq c_{n+j}\}$ as the set of null hypotheses, both being deterministic given the data. Then, we have the decomposition

$$\begin{aligned} \text{FDR}(\mathcal{D}) &= \sum_{k=1}^m \mathbb{E}_{\mathcal{D}} \left[\mathbb{1}\{|\mathcal{S}| = k\} \frac{\sum_{j \in \mathcal{S}^{(1)} \cap \mathcal{H}_0} \mathbb{1}\{\xi \widehat{R}_j \leq k\}}{k} \right] \\ &= \sum_{j \in \mathcal{S}^{(1)} \cap \mathcal{H}_0} \sum_{k=1}^m \mathbb{E}_{\mathcal{D}} \left[\frac{\mathbb{1}\{\xi \widehat{R}_j \leq k\}}{k} (\mathbb{1}\{|\mathcal{S}| \leq k\} - \mathbb{1}\{|\mathcal{S}| \leq k-1\}) \right]. \end{aligned} \quad (22)$$

For any $j \in [m]$, we define $\text{FDR}(\mathcal{D}, j)$ as the summand in (22). Since $|\mathcal{S}| \leq |\mathcal{S}^{(1)}|$ deterministically, we know

$$\mathbb{1}\{\xi \widehat{R}_j \leq k\} (\mathbb{1}\{|\mathcal{S}| \leq k\} - \mathbb{1}\{|\mathcal{S}| \leq k-1\}) = 0$$

for any $k > |\mathcal{S}^{(1)}| =: m_1$. Hence,

$$\text{FDR}(\mathcal{D}, j) = \sum_{k=1}^{m_1} \mathbb{E}_{\mathcal{D}} \left[\frac{1}{k} \mathbb{1}\{\xi \widehat{R}_j \leq k\} \cdot (\mathbb{1}\{|\mathcal{S}| \leq k\} - \mathbb{1}\{|\mathcal{S}| \leq k-1\}) \right]$$

$$\begin{aligned}
&\leq \frac{1}{m_1} + \sum_{k=1}^{m_1-1} \frac{1}{k} \mathbb{E}_{\mathcal{D}} [\mathbf{1}\{\xi \widehat{R}_j \leq k\} \mathbf{1}\{|\mathcal{S}| \leq k\}] - \sum_{k=1}^{m_1-1} \frac{1}{k+1} \mathbb{E}_{\mathcal{D}} [\mathbf{1}\{\xi \widehat{R}_j \leq k+1\} \mathbf{1}\{|\mathcal{S}| \leq k\}] \\
&\leq \frac{1}{m_1} + \sum_{k=1}^{m_1-1} \left\{ \frac{\mathbb{P}_{\mathcal{D}}(\xi \widehat{R}_j \leq k)}{k} \mathbb{P}_{\mathcal{D}}(|\mathcal{S}| \leq k \mid \xi \widehat{R}_j \leq k) - \frac{\mathbb{P}_{\mathcal{D}}(\xi \widehat{R}_j \leq k+1)}{k+1} \mathbb{P}_{\mathcal{D}}(|\mathcal{S}| \leq k \mid \xi \widehat{R}_j \leq k+1) \right\}.
\end{aligned}$$

Here, $\mathbb{P}_{\mathcal{D}}$ is with respect to the conditional distribution of ξ given \mathcal{D} . Now, we would rely on the *positive dependence on a subset* (PRDS) property [Benjamini and Yekutieli, 2001] of $\xi \widehat{R}_j$ as follows to control $\text{FDR}(\mathcal{D}, j)$. For completeness, we include the definition of PRDS below. Lemma B.1 is the same as Lemma C.2 of Jin and Candès [2023b], hence we omit the proof here.

Definition 6 (PRDS). *A random vector $X = (X_1, \dots, X_m)$ is PRDS on a subset \mathcal{I} if for any $i \in \mathcal{I}$ and any increasing set D , the probability $\mathbb{P}(X \in D \mid X_i = x)$ is increasing in x .*

Lemma B.1 (Lemma C.2 of Jin and Candès [2023b]). *Let $a_1, \dots, a_k \in \mathbb{R}$ be nonnegative fixed constants, and let $\xi \sim \text{Unif}([0, 1])$. Then, the random variables $\{a_1\xi, \dots, a_{j-1}\xi, a_{j+1}\xi, \dots, a_k\xi\}$ are PRDS in $a_j\xi$ for any $j \in [k]$.*

By Lemma B.1, we see that

$$\mathbb{P}_{\mathcal{D}}(|\mathcal{S}| \leq k \mid \xi \widehat{R}_j \leq k) \leq \mathbb{P}_{\mathcal{D}}(|\mathcal{S}| \leq k \mid \xi \widehat{R}_j \leq k+1).$$

Since ξ is independent from \widehat{R}_j ,

$$\begin{aligned}
\text{FDR}(\mathcal{D}, j) &\leq \frac{1}{m_1} + \sum_{k=1}^{m_1-1} \left\{ \frac{\mathbb{P}_{\mathcal{D}}(\xi \widehat{R}_j \leq k)}{k} - \frac{\mathbb{P}_{\mathcal{D}}(\xi \widehat{R}_j \leq k+1)}{k+1} \right\} \mathbb{P}_{\mathcal{D}}(|\mathcal{S}| \leq k \mid \xi \widehat{R}_j \leq k) \\
&= \frac{1}{m_1} + \sum_{k=1}^{m_1-1} \left\{ \frac{\min\{1, k/\widehat{R}_j\}}{k} - \frac{\min\{1, (k+1)/\widehat{R}_j\}}{k+1} \right\} \mathbb{P}_{\mathcal{D}}(|\mathcal{S}| \leq k \mid \xi \widehat{R}_j \leq k)
\end{aligned}$$

If $\widehat{R}_j \geq m_1$, both minimum term evaluate to $1/\widehat{R}_j$, leading to $\text{FDR}(\mathcal{D}, j) \leq \frac{1}{m_1} \leq \frac{1}{\widehat{R}_j}$. Otherwise,

$$\begin{aligned}
\text{FDR}(\mathcal{D}, j) &\leq \frac{1}{m_1} + \sum_{k=\widehat{R}_j}^{m_1-1} \left\{ \frac{1}{k} - \frac{1}{k+1} \right\} \mathbb{P}_{\mathcal{D}}(|\mathcal{S}| \leq k \mid \xi \widehat{R}_j \leq k) \\
&\leq \frac{1}{m_1} + \sum_{k=\widehat{R}_j}^{m_1-1} \left\{ \frac{1}{k} - \frac{1}{k+1} \right\} = \frac{1}{\widehat{R}_j}.
\end{aligned}$$

Putting above bounds together, we have

$$\text{FDR}(\mathcal{D}) \leq \sum_{j \in \mathcal{S}^{(1)} \cap \mathcal{H}_0} \frac{1}{\widehat{R}_j} = \sum_{j=1}^m \frac{\mathbf{1}\{p_j \leq s_j, Y_{n+j} \leq c_{n+j}\}}{\widehat{R}_j}.$$

Finally, marginalizing over the randomness in \mathcal{D} concludes the proof of the homogeneous case.

Case 3: Deterministic pruning. In this case, we have

$$\mathcal{S} = \{j : p_j \leq s_j, \widehat{R}_j \leq r^*\} \quad \text{and} \quad r^* = |\mathcal{S}|.$$

by Proposition A.1. Therefore, for any $j \in \mathcal{S}$, we have $\widehat{R}_j \leq |\mathcal{S}|$, and

$$\begin{aligned} \text{FDR} &= \mathbb{E} \left[\frac{\sum_{j=1}^m \mathbf{1}\{j \in \mathcal{S}, Y_{n+j} \leq c_{n+j}\}}{1 \vee |\mathcal{S}|} \right] \leq \mathbb{E} \left[\frac{\sum_{j=1}^m \mathbf{1}\{j \in \mathcal{S}, Y_{n+j} \leq c_{n+j}\}}{\widehat{R}_j} \right] \\ &\leq \mathbb{E} \left[\frac{\sum_{j=1}^m \mathbf{1}\{p_j \leq s_j, Y_{n+j} \leq c_{n+j}\}}{\widehat{R}_j} \right]. \end{aligned}$$

This concludes the proof of the deterministic case and hence also the proof of Lemma 3.3. \square

C Additional details and results for numerical experiments

C.1 Simulation setups for Section 5.1

For Liang’s settings, the configuration of X_i , θ_i and ϵ_i for $i \in [d]$ are summarized in Table 1. The feature dimension is taken to be $d = 300$ and the noise level is taken to be $\sigma = 3$. The degree of freedom used in t -distribution is $\nu = 3$. The regression function is defined as $\mu(x) = X_i^\top \theta_i$.

Setting	X_i	θ_i	ϵ_i
1	$\mathcal{N}(0, \mathbf{I}_d)$	$\mathbf{1}\{i \bmod 20 = 0\}$	$\sigma \cdot \mathcal{N}(0, 1)$
2	$\mathcal{N}(0, \mathbf{I}_d)$	$\mathbf{1}\{i \bmod 20 = 0\}$	$\sigma \cdot t_\nu(1)$
3	$\mathcal{N}(0, \mathbf{I}_d)$	$1/d$	$\sigma \cdot \mathcal{N}(0, 1/d)$
4	$t_\nu(0, \mathbf{I}_d)$	$\mathbf{1}\{i \bmod 20 = 0\}$	$\sigma \cdot \mathcal{N}(0, 1)$

Table 1: Details of the four data generating processes used in Liang’s settings.

In Liang’s settings, we consider eleven combinations of models and scores for the model/score selection process. Following the setups in Liang et al. [2024a], we fit nine linear conditional quantile regression models at quantiles $\alpha \in \{0.1, 0.2, \dots, 0.9\}$ using a randomly selected subset of features of size $d/10$. For these models, the conformity score used is $M \cdot \mathbf{1}\{Y > c\} - \widehat{q}_\alpha(x)$ with $M = 100$, where \widehat{q}_α is the fitted quantile regression model at level α . The remaining two model options are a shared linear model $\widehat{\mu}(\cdot)$ estimating the conditional mean of Y given X , fitted using $d/5$ randomly selected features, with two choices of conformity scores: the standard clipped score $M \cdot \mathbf{1}\{Y > c\} - \widehat{\mu}(x)$ and a studentized version $M \cdot \mathbf{1}\{Y > c\} - \widehat{\mu}(x)/\widehat{\sigma}(x)$ with $M = 1000$, where $\widehat{\sigma}$ is a linear conditional standard error model estimating the absolute prediction error $\mathbb{E}[|Y - \widehat{\mu}(x)| \mid X = x]$. The conditional standard deviation model $\widehat{\sigma}$ is trained on an additional dataset of 100 observations (since all methods have access to the same set of pre-trained model, the comparison is still fair). All the models are fitted using functions in the `scikit-learn` Python package. In this setting, the quality of models mainly depends on how many “true” features are included in the regression modeling.

The details for Jin’s settings are summarized in Table 2. In Section 5.1, we set the feature dimension at $d = 20$, and the noise level at $\sigma = 1$. Settings (1,3) and (2,4) have the same regression function, yet with different heterogeneity structure in the noise distribution.

For Jin’s settings, we consider 24 options for the combination of prediction models and scores. We fitted random forest (using the `quantile-forest` Python package) and gradient boosting (using the `scikit-learn` Python package) quantile regressors at nine quantile levels $\alpha \in \{0.1, 0.2, \dots, 0.9\}$, yielding 18 models. For these models, the conformity score is defined as $V(x, y) = M \cdot \mathbf{1}\{Y > c\} - \widehat{q}_\alpha(x)$ with $M = 1000$. Additionally, we fit a random forest conditional mean model (with `scikit-learn` Python package), $\widehat{\mu}$, which is shared across the remaining six model options. These six options use conformity scores of the form $M \cdot \mathbf{1}\{Y > c\} - \widehat{\mu}(x)/\widehat{\sigma}(x)$ with $M = 1000$ and 6 options for the function $\widehat{\sigma}(\cdot)$: a constant value of 1 (equivalent to the standard clipped score) and five conditional mean squared error models, including gradient boosting,

Setting	X_i	$\mu(\cdot)$	ϵ_i
1	$\text{Unif}[0, 1]^d$	$4x_1 \mathbb{1}\{x_2 > 0\} \cdot \max\{0.5, x_3\} + 4x_1 \mathbb{1}\{x_2 \leq 0\} \cdot \min\{x_3, -0.5\}$	$\sigma \cdot \mathcal{N}(0, 1)$
2	$\text{Unif}[0, 1]^d$	$2(x_1 x_2 + e^{x_4} - 1)$	$\frac{3}{2}\sigma \cdot \mathcal{N}(0, 1)$
3	$\text{Unif}[0, 1]^d$	$4x_1 \mathbb{1}\{x_2 > 0\} \cdot \max\{0.5, x_3\} + 4x_1 \mathbb{1}\{x_2 \leq 0\} \cdot \min\{x_3, -0.5\}$	$\sigma \cdot (5.5 - \mu(x))/2$
4	$\text{Unif}[0, 1]^d$	$2(x_1 x_2 + e^{x_4} - 1)$	$\sigma \cdot (5.5 - \mu(x))/2$

Table 2: Details of the four data generating processes used in Jin’s settings.

random forest, support vector machine, Lasso, and Ridge regression, all using the `scikit-learn` package. The model $\hat{\sigma}$ is trained on an additional dataset of 100 observations.

C.2 Additional results for Section 5.1

In this part, we include additional simulation results that show the performance of OptCS-MSel and baselines when the training and calibration sample sizes vary. Figure 14 presents the empirical FDR and power for Liang’s settings, and Figure 15 presents these results for Jin’s settings.

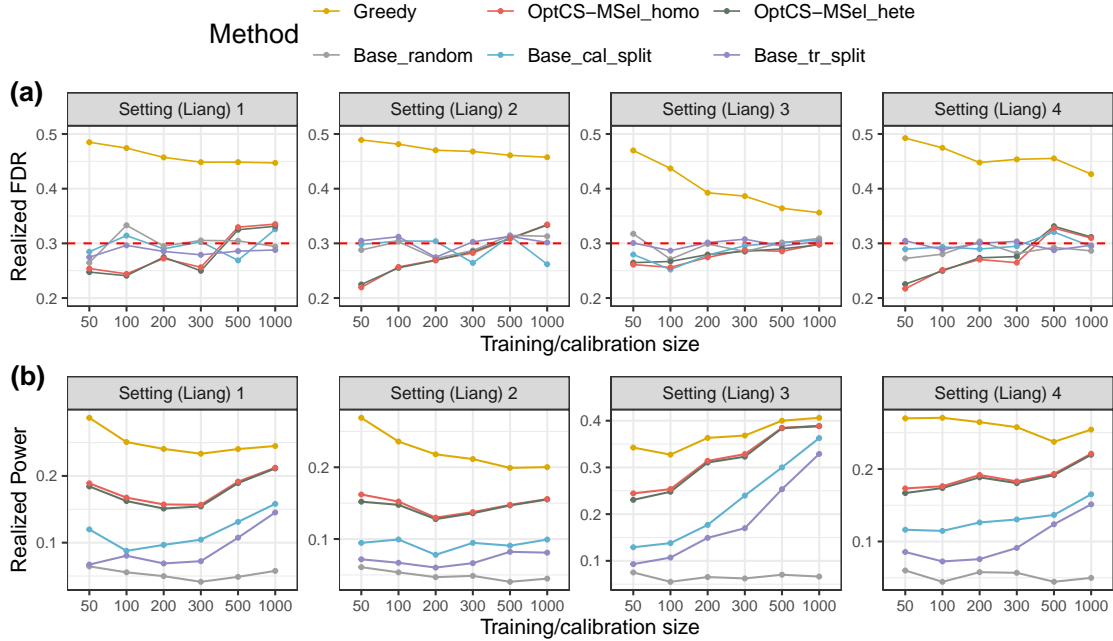


Figure 14: Additional results for Section 5.1 when varying sample sizes for Liang’s settings. Each subplot corresponds to one data generating process, with x -axis being $n = n_{\text{train}} = n_{\text{calib}}$, while fixing $q = 0.3$.

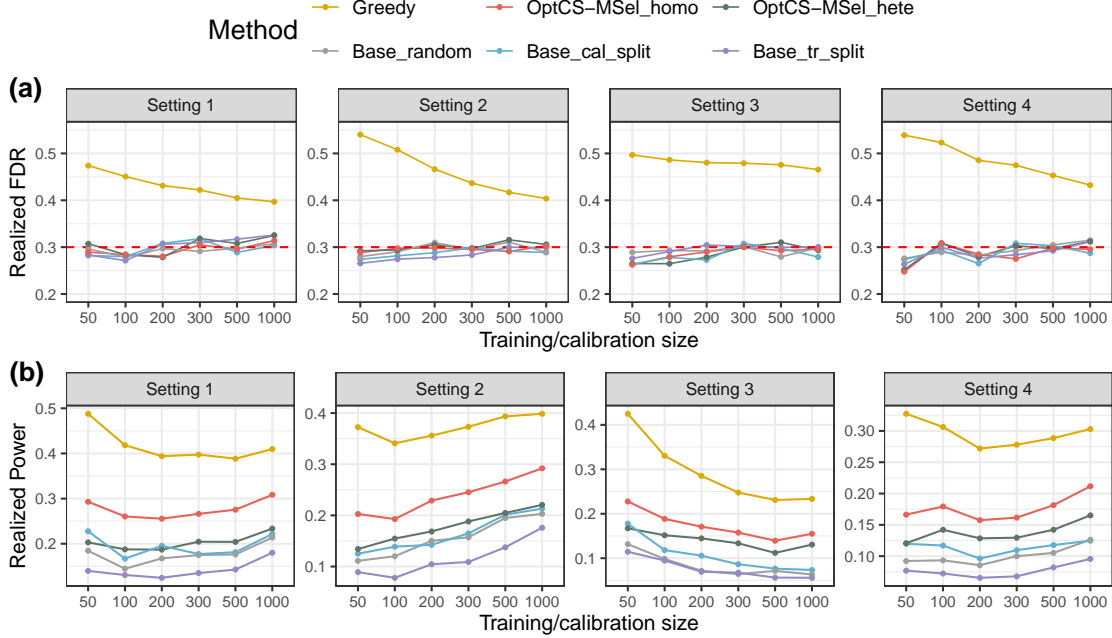


Figure 15: Additional results for experiments in Section 5.1 when varying sample sizes for Jin’s settings. Details are otherwise the same as Figure 14.

C.3 Simulation setups for Section 5.2

The details for Jin’s settings used in Section 5.2 can be found in Table 3. We adapt the settings from Jin and Candès [2023b] to a classification setting, where the binary labels are defined via $Y_i = \mathbf{1}\{\mu(X_i) + \epsilon_i > 0\}$. The feature dimension is $d = 10$ to limit the computation costs, and the noise level is $\sigma = 0.5$. In Table 3, the settings 1 and 3 slightly modify the settings 1 and 3 in Table 2 to make sure that increasing the training sample size leads to more powerful models at least in the split conformal selection procedure. We note that in the original settings 1 and 3 in Table 2, increasing the sample size reduces selection power in SCS potentially due to the specific choice function classes, yet this does not affect the results in Section 5.1 since the sample sizes are fixed there. We will thus use these four settings for both Section 5.2 and Section 5.3.

Setting	X_i	$\mu(\cdot)$	ϵ_i
1	$\text{Unif}[0, 1]^d$	$\frac{1}{2} \mathbf{1}\{x_1 x_2 > 0\} + \mathbf{1}\{x_1 x_2 \leq 0\} + x_4$	$2\sigma \cdot \mathcal{N}(0, 1)$
2	$\text{Unif}[0, 1]^d$	$2(x_1 x_2 + e^{x_4} - 1)$	$\frac{3}{2}\sigma \cdot \mathcal{N}(0, 1)$
3	$\text{Unif}[0, 1]^d$	$\frac{1}{2} \mathbf{1}\{x_1 x_2 > 0\} + \mathbf{1}\{x_1 x_2 \leq 0\} + x_4$	$\sigma \cdot (5.5 - \mu(x))/2$
4	$\text{Unif}[0, 1]^d$	$2(x_1 x_2 + e^{x_4} - 1)$	$\sigma \cdot (5.5 - \mu(x))/3$

Table 3: Details of the four data generating processes used in Jin’s settings for Section 5.2.

C.4 Additional results for Section 5.2

Figure 16 presents the empirical FDR and power for all three model classes (random forest and support vector regression using `scikit-learn` Python library, and XGBoost using `xgboost` Python library) considered in

Jin and Candès [2023c] for the four data generating processes. Consistent with the results in Section 5.2, OptCS-Full outperforms sample splitting baselines by utilizing all sample in training. Moreover, the over-sampling and separate-training variants yield similar performance.

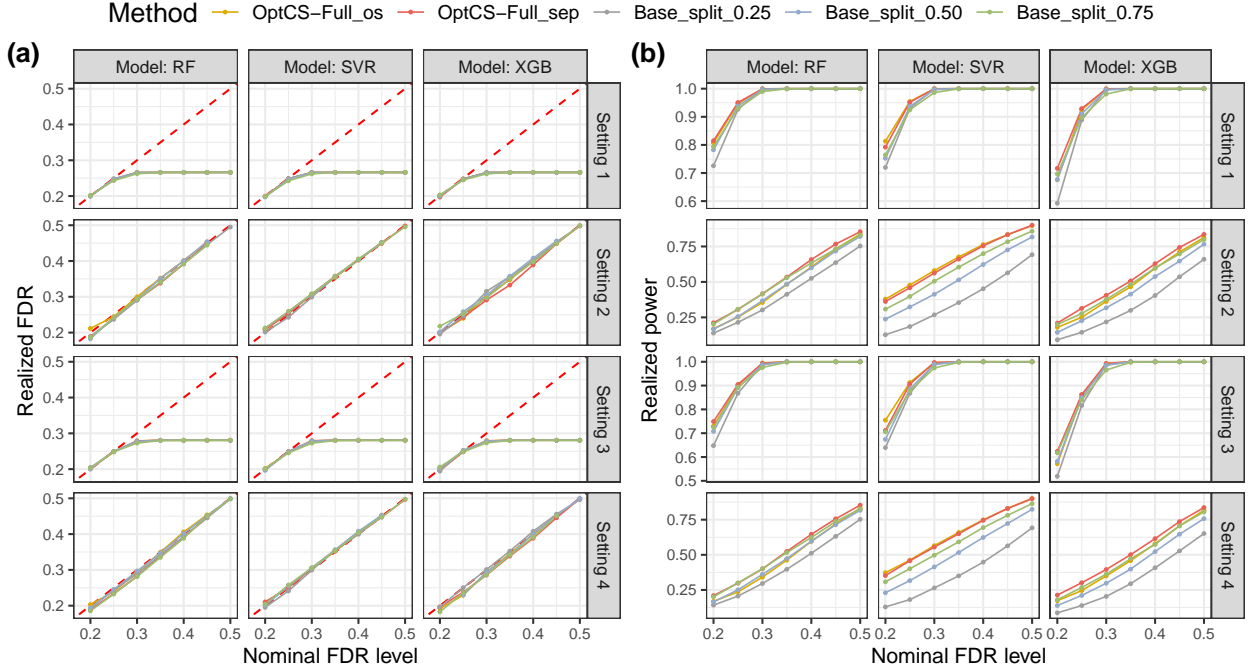


Figure 16: Results for OptCS-Full and split conformal selection with all three model classes: random forest, support vector regression and gradient boosting. Details are the same as Figure 8.

C.5 Simulation setups for Section 5.3

In this section, we use the same data-generating processes as in C.1 for Liang’s settings and C.3 for Jin’s settings. To repeat the coefficients again, we use a feature dimension of $d = 10$, and noise level $\sigma = 0.5$ for Jin’s settings. For Liang’s settings, we use feature dimension $d = 300$, noise level $\sigma = 3$, and degree of freedom $\nu = 3$ for the t -distributions involved in the data generation.

For Liang’s settings, we consider 7 combinations of models and scores. Three linear conditional quantile models at quantile level $\alpha = 0.25, 0.5, 0.75$ were fitted using randomly selected subset of features of size $d/10$. Similar to setups in section C.1, the conformity scores used here takes the form $V(x, y) = M \cdot \mathbf{1}\{Y > c\} - \hat{q}_\alpha(x)$ for $M = 1000$. For the remaining 4 options, we fit two linear regression models with $d/10$ and $d/5$ randomly chosen features, and pair them with either an linear regression error model $\hat{\sigma}$ or without error estimation, i.e. $\hat{\sigma} \equiv 1$. In the case where an error model is employed, the set of all labeled data is first partitioned to two subsets for fitting the linear regression model (70%) and the error model (30%) in the first place, respectively. The conformity scores for these options are $M \cdot \mathbf{1}\{Y > c\} - \hat{\mu}(x)/\hat{\sigma}(x)$ for $M = 1000$. All these models are fitted using functions in the `scikit-learn` Python package. As we adopt two options with $d/5$ features as supposed to $d/10$, the model accuracies vary significantly in this setting. This explains the relatively big performance gap between the random baselines and other competing methods.

For Jin’s settings, we consider 9 pairs of candidate model and scores. We fitted three random forest quantile regressions at level $\alpha = 0.25, 0.5, 0.75$ (from `quantile-forest` package), and again use conformity scores of the form $V(x, y) = M \cdot \mathbf{1}\{Y > c\} - \hat{q}_\alpha(x)$. We also consider 3 conditional mean models: support vector regression, Lasso and Ridge regression. Each of them is paired with either a conditional error model $\hat{\sigma}$ fitted with SVR or without error estimation (i.e., the clipped score). Again, the conformity scores for these

options are $M \cdot \mathbb{1}\{Y > c\} - \hat{\mu}(x)/\hat{\sigma}(x)$, and when an error model is used, a 70%-30% data split is done to train the conditional mean model and error model respectively.

C.6 Datasets and pre-trained model for Section 6.2

In Section 6.2, we use the same subset (p10, p11 and p12 folders) of the MIMIC-CXR dataset [Johnson et al., 2019] as in Gui et al. [2024], which is accessed from the PhysioNet project page <https://physionet.org/content/mimic-cxr/2.0.0/> under the PhysioNet Credentialed Health Data License 1.5.0. In our experiments, we draw a subset of images in the test folder determined by the same split as Gui et al. [2024]. In this way, the randomness is purely from randomly splitting the data into labeled data and test samples.

The foundation model for generating the radiology reports is the one fine-tuned in Gui et al. [2024]. We include the details here for completeness. Specifically, this vision-language model combines the Vision Transformer `google/vitbase-patch16-224-in21k` pre-trained on ImageNet-21k⁴ as the image encoder and GPT2 as the text decoder. Each raw image is resized to 224×224 pixels. The model is fine-tuned on a hold-out dataset with a sample size of 43,300 for 10 epochs with a batch size of 8, and other hyperparameters are set to default values. When generating reports, all the parameters are kept the same as the conformal alignment paper; we refer the readers to [Gui et al., 2024, Appendix C.2] for these details.

C.7 Detailed setup for Section 6.2

We use exactly the same procedures as Gui et al. [2024] to compute 12 features which (heuristically) measure the uncertainty of LLM-generated outputs:

- *Input uncertainty scores* (`Lexical_Sim`, `Num_Sets`, `SE`). Following Kuhn et al. [2023], we compute a set of features that measure the uncertainty of each LLM input through similarity among multiple answers. The features include lexical similarity (`Lexical_Sim`), the rouge-L similarity among the answers. In addition, we use a natural language inference (NLI) classifier to categorize the M answers into semantic groups, and compute the number of semantic sets (`Num_Sets`) and semantic entropy (`SE`). Following Kuhn et al. [2023], Lin et al. [2023], we use an off-the-shelf DeBERTa-large model [He et al., 2020] as the NLI predictor.
- *Output confidence scores* (`EigV(J/E/C)`, `Deg(J/E/C)`, `Ecc(J/E/C)`). We also follow [Lin et al., 2023] to compute features that measure the so-called output confidence: with M generations, we compute the eigenvalues of the graph Laplacian (`EigV`), the pairwise distance of generations based on the degree matrix (`Deg`), and the Eccentricity (`Ecc`) which incorporates the embedding information of each generation. Note that each quantity is associated with a similarity measure; we follow the notations in Lin et al. [2023] and use the suffix J/E/C to differentiate similarities based on the Jaccard metric, NLI prediction for the entailment class, and NLI prediction for the contradiction class, respectively.

For experiments with OptCS-Full, we consider three model classes, logistic regression and random forests from the `scikit-learn` Python library and XGBoost from the `xgboost` Python library, utilizing all the above measures as the features.

The first setup in experiments with OptCS-Full-MSel is as follows. We treat the task as a regression problem, and fit 3 linear quantile regressors and 3 random forest quantile regressors at quantile level $\alpha = 0.25, 0.5, 0.75$. They are paired with the conformity score $V(x, y) = My - \hat{q}_\alpha(x)$ with $M = 1000$. For the remaining 6 options, we use conformity score of the form $My - \hat{\mu}(x)/\hat{\sigma}(x)$, where $\hat{\mu}$ is taken to be a random forest model, support vector regression model or linear regression model. Each of them is paired with no error estimation, i.e. $\hat{\sigma} \equiv 1$, or a Lasso error model fitted using 70% of the total training data.

The second setup for OptCS-Full-MSel experiments is as follows. We group the features into four groups:

⁴<https://huggingface.co/google/vit-base-patch16-224-in21k>

- (a) Input uncertainty scores: (`Lexical_Sim`, `Num_Sets`, `SE`).
- (b) Output confidence scores with Jaccard metric: (`EigV(J)`, `Deg(J)`, `Ecc(J)`).
- (c) Output confidence scores with NLI prediction for entailment: (`EigV(E)`, `Deg(E)`, `Ecc(E)`).
- (d) Output confidence scores with NLI prediction for contradiction: (`EigV(C)`, `Deg(C)`, `Ecc(C)`).

We train three classification model classes (logistic regression, random forest, and XGBoostRF, using the `scikit-learn` and `xgboost` Python library) with each individual group of features and all four groups of features, respectively, leading to a total of 15 classification models g . Then, we use the same conformity score $V(x, y) = My - g(x)$ for $M = 1000$.

The baselines considered in above two setups are very similar to those in Section 5.3. For clarity, we summarize them again here:

- (i). `OptCS-Full-MSel`: Our OptCS-Full-MSel procedure where the training process uses over-sampling.
- (ii). `Greedy`: Randomly split the labeled data into $\mathcal{D}_{\text{train}}$ (62.5%) and $\mathcal{D}_{\text{calib}}$ (37.5%). After training each candidate model on $\mathcal{D}_{\text{train}}$, we use the conformity score function which leads to the largest selection set in SCS, with $\mathcal{D}_{\text{calib}}$ as the calibration data. This configuration of data splitting is to agree with the ratio suggested in Gui et al. [2024].
- (iii). `Base_random`: Split the data with the same ratio as in (ii), and then apply SCS with a randomly chosen model.
- (iv). `Base_split_112`: Randomly split the labeled data into $\mathcal{D}_{\text{train}}$, \mathcal{D}_{sel} , and $\mathcal{D}_{\text{calib}}$ with ratio 1:1:2. We use $\mathcal{D}_{\text{train}}$ to train all the models, use \mathcal{D}_{sel} to run SCS (after additional splitting) and select the model with largest selection set, then use $\mathcal{D}_{\text{calib}}$ to run SCS with the test data and the selected model.
- (v). `Base_split_121`: Similar to (iii), with data split ratio 1:2:1 for $\mathcal{D}_{\text{train}}$, \mathcal{D}_{sel} , and $\mathcal{D}_{\text{calib}}$.
- (vi). `Base_split_211`: Similar to (iii), with data split ratio 2:1:1 for $\mathcal{D}_{\text{train}}$, \mathcal{D}_{sel} , and $\mathcal{D}_{\text{calib}}$.
- (vii). `Base_split_111`: Similar to (iii), with data split ratio 1:1:1 for $\mathcal{D}_{\text{train}}$, \mathcal{D}_{sel} , and $\mathcal{D}_{\text{calib}}$.